

DESIGN OF MICROWAVE PRINTED CIRCUIT

LOG - PERIODIC ANTENNAS

DESIGN OF MICROWAVE PRINTED CIRCUIT

LOG - PERIODIC ANTENNAS

by

Hugo Kneve, B. Eng.

A Thesis

Submitted to the Faculty of Graduate Studies

in Partial Fulfillment of the Requirements

for the Degree

Master of Engineering

McMaster University

November, 1977.

Master of Engineering (1977)

McMaster University

(Electrical Engineering)

Hamilton, Ontario.

Title: Design of Microwave Printed Circuit

Log - Periodic Antennas

Author: Hugo Kneve, B. Eng. (McMaster)

Supervisor: Dr. C. K. Campbell.

Number of Pages: (x), 101

Scope and Contents:

A method for designing antennas whose characteristics are independent of frequency within a certain specified arbitrary band as given by Robert L. Carrel is modified to facilitate design in the microwave region using printed circuit techniques. A simplified theory of antenna operation is presented and design procedures required to manufacture the devices are given.

A typical design and actual results of antenna performance are given.

ABSTRACT

The subject presented in this thesis concerns the design and fabrication of microwave printed circuit log - periodic antennas meant for operation at frequencies above 1.0 GHz. The designs has its basis in the work which was presented by Robert L. Carrel as a Ph.D. thesis in 1961 and is one of the classic papers in the design of log - periodic dipole arrays.

The method is modified to some extent firstly to compensate for planar, instead of cylindrical dipole and the effect of dielectric loading which the supporting substrate provides.

Methods which allow feeding the array from the opposite direction in which the main lobe extends are also discussed, one of which, the mode converter, is found to be immediately successful.

A typical antenna is fabricated, its input impedance and radiation pattern measured and the results discussed with some comparison to Carrel's results.

ACKNOWLEDGEMENTS

Firstly, the author would like to express his appreciation toward Dr. C. K. Campbell who, while acting as supervisor for this thesis, provided numerous insights toward antenna theory and proper techniques for measuring microwave devices.

Thanks are also expressed to Dr. S. S. Haykin, Director of the Communications Research Laboratory at McMaster University for allowing the use of the facilities at C.R.L. The author is also greatly indebted to his colleagues, Mr. M. S. Suthers, Mr. D. Seiler, Mr. J. P. Reilly and Mr. S. Nanayakkara for their comments during numerous discussions concerning certain aspects of the research.

Thanks are extended to Mr. P. Edmonson whose technical aid and advice often proved to be very helpful.

This research was supported in part by a research grant provided by the National Research Council of Canada to whom appreciation is expressed.

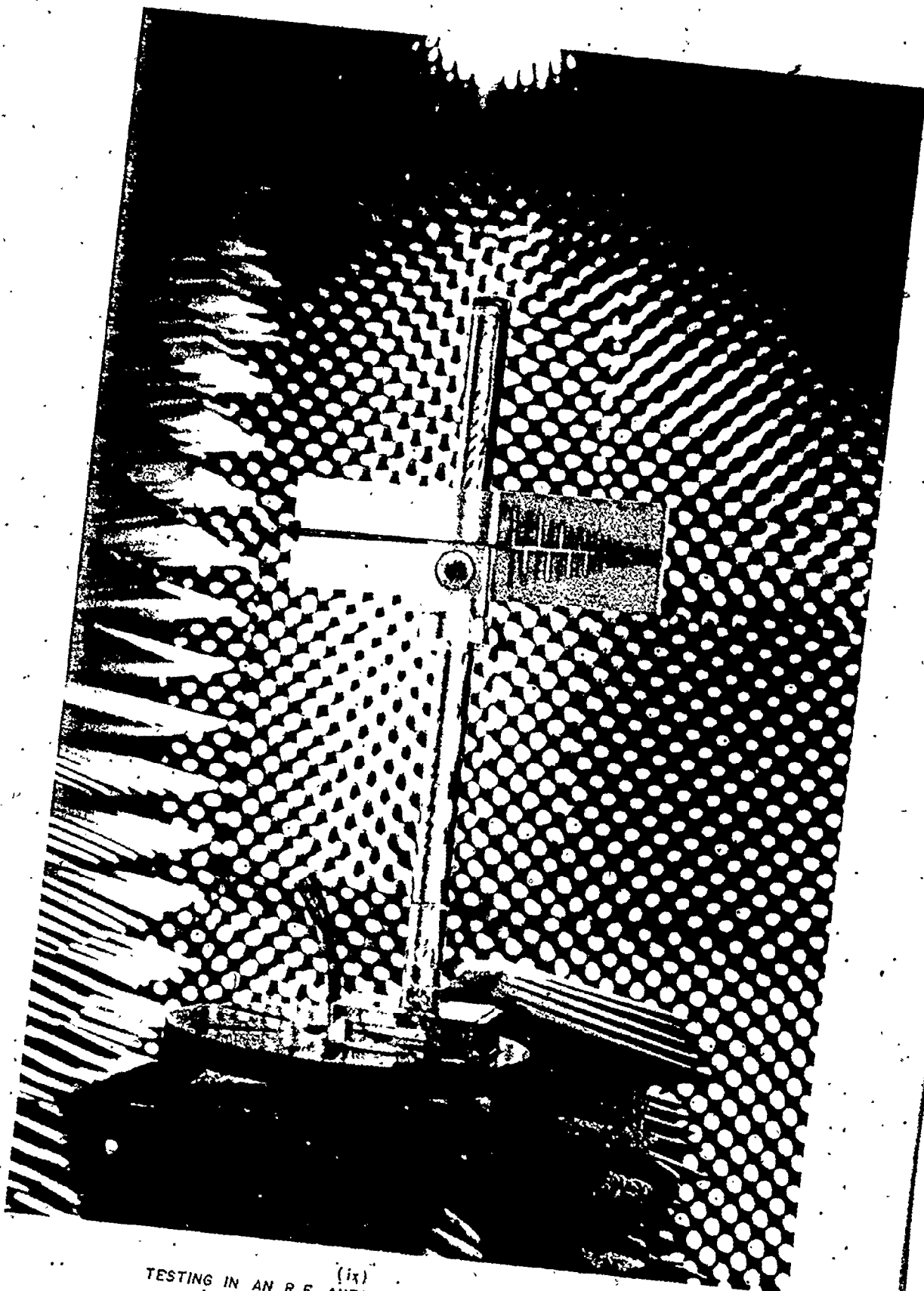
<u>TABLE OF CONTENTS</u>	<u>PAGE</u>
CHAPTER I: INTRODUCTION	1
1.1 Scope of Thesis	1
1.2 General Considerations	1
CHAPTER II: THEORY OF LOGARITHMICALLY PERIODIC ANTENNAS	6
2.1 Evolution of the Log-Periodic Dipole Array	6
2.2 LPDA Theory of Operation	13
2.3 LPDA Design Procedure	23
2.4 Terminal Impedance of the LPDA	31
2.5 Summary	38
CHAPTER III: FEED MECHANISMS FOR THE LPDA	40
3.1 Necessity for a Balun	40
3.2 Frequency Independent Baluns	43
CHAPTER IV: DESIGN AND PERFORMANCE OF AN M.P.C. LOG - PERIODIC DIPOLE ARRAY	50
4.1 General	50
4.2 Determination of Dipole Impedance and Extent of Dielectric Loading	50
4.3 Design of a C - Band LPDA	59
4.4 Testing of the Baluns	65
4.5 Design of S - Band LPDA with Mode Converter Feed	73
CHAPTER V: CONCLUSIONS	85
APPENDIX A	87
APPENDIX B	89
APPENDIX C	92
APPENDIX D	98

<u>LIST OF FIGURES</u>	<u>PAGE</u>
Figure 2.1 Equi - angular spiral antenna	7
Figure 2.2 Planar log - periodic antenna	9
Figure 2.3 Log - periodic dipole array	12
Figure 2.4 LPDA geometry	14
Figure 2.5 Unsuccessful and successful feeds for LPDA	16
Figure 2.6 Line array of isotropic sources	18
Figure 2.7 Transmission line model for the LPDA	22
Figure 2.8 Voltages and currents along LPDA (after Carrel)	24
Figure 2.9 Nomogram	32
Figure 2.10 Nomogram	33
Figure 2.11 Nomogram	34
Figure 3.1 Balanced & unbalanced modes on coaxial line	41
Figure 3.2 Effect of directly attaching a dipole to coaxial line and equivalent circuit	42
Figure 3.3 Self - balun method for feeding LPDA	45
Figure 3.4 Coaxial and microstrip mode converters	47
Figure 3.5 Reflection balun geometry	48
Figure 4.1 Half wave dipole fed from mode converter	51
Figure 4.2 Mode converter before & after compensation	55
Figure 4.3 S_{11} response of a half wave dipole for varying h/w	56
Figure 4.4 Dipole characteristic impedance vs. h/w	57
Figure 4.5 C - band LPDA fed from mode converter	62
Figure 4.6a S_{11} response 5.9 - 9.0 GHz.	63

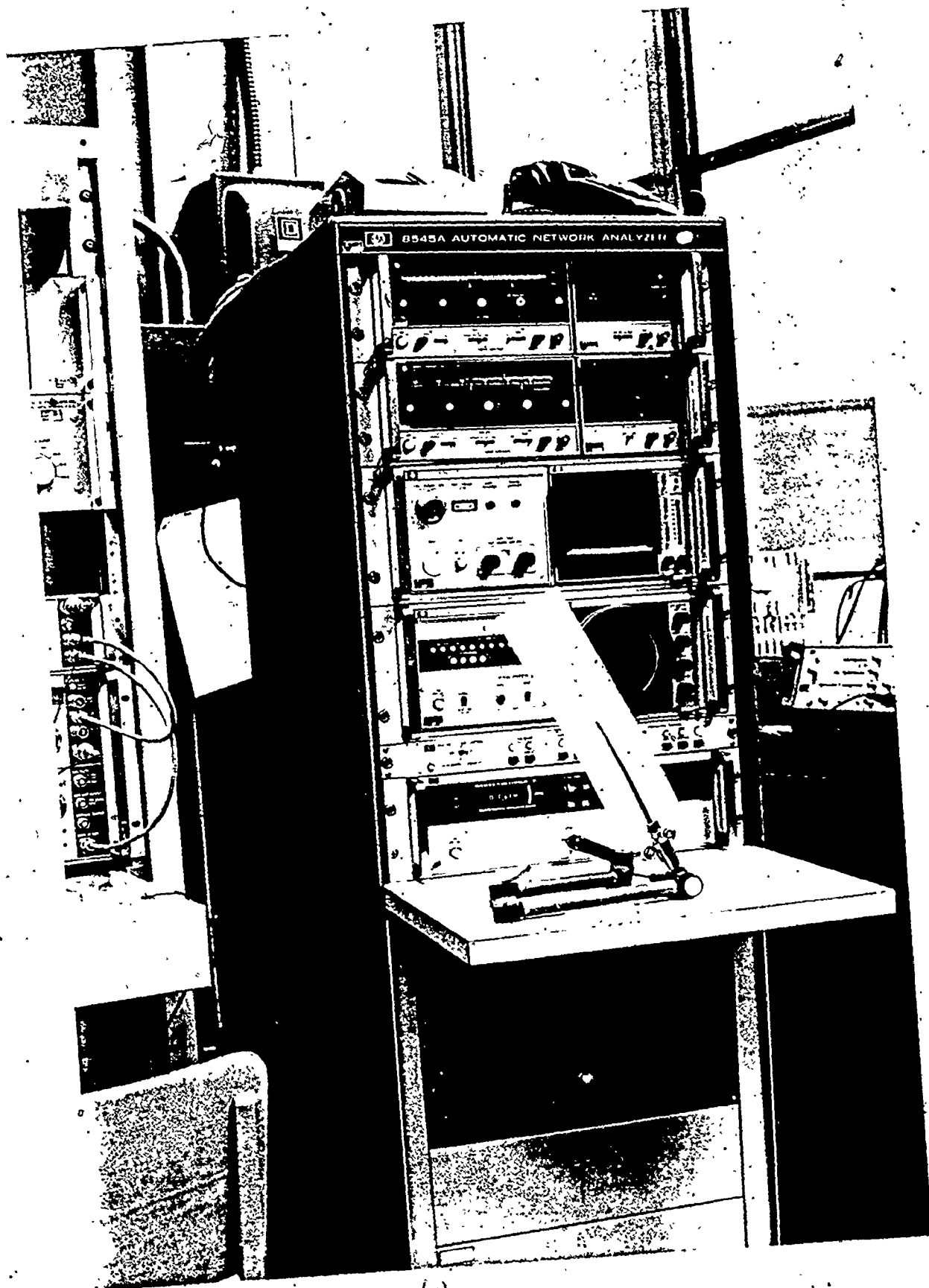
	<u>PAGE</u>
Figure 4.6b S_{11} response 8.0 - 12.4 GHz.	64
Figure 4.7 Voltages with respect to ground on balanced line of 100 MHz. reflection balun	66
Figure 4.8 Reflection from 50 & 200 ohm lines	67
Figure 4.9 Voltage & current distributions of incident and reflected waves on the reflection balun	69
Figure 4.10 Mode converter feed for LPDA	72
Figure 4.11 Reduction of balanced line impedance when sandwiched between conducting planes	74
Figure 4.12 S_{11} response 1.8 - 4.2 GHz.	77
Figure 4.13 S_{11} response 1.8 - 4.2 GHz.	78
Figure 4.14 H - plane radiation patter for S - band LPDA (0° - 90°)	79
Figure 4.15 H - plane radiation pattern for S - band LPDA (100° - 180°)	80
Figure 4.16 E - plane radiation pattern for S - band LPDA (0° - 90°)	81
Figure 4.17 E - plane radiation pattern for S - band LPDA (100° - 180°)	82
Figure C - 1 Microstrip characteristic impedance calcu- lated from work of Wheeler	93
Figure C - 2 Balanced line impedance	94
Figure C - 3 Balanced line impedance	95
Figure C - 4 Balanced line impedance	96

Figure C - 5 Graph of $\sqrt{\epsilon_r} Z_0$ vs. W/b for various values
of t/b

97



(ix)
TESTING IN AN R.F. ANECHOIC CHAMBER



(x)
AUTOMATIC NETWORK ANALYZER SYSTEM

CHAPTER I

INTRODUCTION

1.1 Scope of the Thesis:

The primary objective of this thesis is to design, fabricate and test a microwave printed circuit log-periodic antenna. Although the log-periodic antenna has been in existence for some twenty years, all of the reported designs have been for structures in the H.F., V.H.F., and some in the U.H.F. regions of the radio spectrum. Because of the relatively long wavelengths involved, as compared to the microwave region, these structures were composed of cylindrical dipole elements suitably arranged in a log-periodic fashion and suspended in free space.

The concept presented in this thesis is that one can take the traditional methods for designing a log-periodic antenna and, with suitable modifications, construct an analogous structure out of copper-clad dielectric board.

Topics included in the discussion are the effect of the dielectric on the characteristic impedance and resonant frequency of a half-wave dipole antenna, effect of the dielectric on the terminal impedance of the dipole array, methods of feeding the antenna array, and a detailed outline on how to produce a log-periodic dipole antenna array.

1.2 General Considerations:

Until recently, radio antennae have been considered to be quite frequency selective in their response to an incident R.F. wave

regardless of the type of antenna or its configuration. Notably, one may observe the case of a simple half-wave dipole antenna and its cousin, the Yagi-Uda array. In this instance, the relatively sharp resonance of the dipole is replaced with a more broadband response through the addition of parasitic director and reflector elements. Although one may consider the Yagi as a fairly broadband device, it must be remembered that there is a practical limit as to how far the array may be broadbanded without sacrificing performance in the form of pattern breakup and degradation of input impedance as a function of frequency. Other antenna types such as the rhombic and discone (1) have useable bandwidths of up to four to one but still remain band limited.

The problem of band limited antennas remained until 1957 when V.H. Rumsey introduced the notion of a frequency-independent antenna. The idea which was presented was that if an antenna structure could be described entirely by angles rather than depend on any length dimension, it would have characteristics such as input impedance, polarization and far field pattern which are independent of frequency. The only inherent problem with this idea was that all of these structures must extend to infinity in order to be truly frequency independent, and some structures, notably the biconical antenna, were seen to suffer greatly in their characteristics when truncated to finite length. One therefore had to be satisfied with an antenna which was quasi-frequency independent; that is to say: a structure whose bandwidth is not infinite but may be arbitrarily chosen through constraints set by the designer and the upper and lower

frequency limits being determined by the truncation of the device.

Several successful frequency independent structures have been constructed based on Rumsey's premise. Included among these antennas are the planar- and conical-equiaxial spiral, planar- and non-planar log-periodic antenna, log-periodic dipole and log-periodic monopole arrays (2). The log-periodic dipole (L.P.D) and log-periodic monopole (L.P.M) have several variations based on them including the log-periodic wire trapezoid (based on the L.P.D.) and bent log-periodic zig-zag (based on the L.P.M.) (2).

In 1961, Robert L. Carrel presented a paper which concerned itself with the analysis of the operation of the log - periodic dipole array (L.P.D.A.) and gave quantitative results for antenna performance as a function of array parameters (3). Since the appearance of the paper, much interest ensued toward establishing the feasibility of using the L.P.D.A. in military (4,16), industrial/research, and consumer applications.

One must consider, however, that as one extends the operating frequency of a system into the microwave region ($f > 900$ MHz.) the construction of a free space dipole array becomes exceedingly difficult at frequencies in excess of 2 GHz. In this thesis, it is proposed that the problem of accurate formation and placement of small dipoles in the array can be resolved by resorting to a printed circuit technique in which the dipole elements are chemically etched from a copper-clad dielectric board. Although the problem of constructing and supporting the array may be solved in this manner, it is important

to note that the array is no longer contained in a homogeneous medium, namely free space, but rather in an inhomogeneous medium consisting of both the surrounding space and the supporting dielectric substrate. The presence of this dielectric becomes the source of some rather annoying side effects on antenna performance. Firstly, the presence of a dielectric within an electric field will cause the electric lines of force to be contained to some extent within the dielectric, the amount of containment being proportional to the relative dielectric permittivity. Consequently the near field of an antenna array and, as a result, the far field distribution are changed, in some degree, from their shape in free space. Secondly, if one regards a dipole as an opened out transmission line, the added dielectric increases the capacitance between the monopole elements, thereby reducing the terminal impedance of the dipole as well as making it look longer electrically than its physical dimension would dictate.

Since one would only be concerned with using one particular dielectric throughout an antenna design, it is sufficient, for the purpose of this thesis, to experimentally determine the input impedance of a dielectrically supported dipole as a function of its monopole length to width ratio. While making these measurements, one may also note the resonant frequency of the dipole with respect to its free space resonance. Thus, one may determine at the same time how much to scale down the dipoles in order to maintain the desired pass band when one designs the array.

Having designed the array, one is still left with the problem of properly feeding the structure from either the receiver or transmitter with a suitably balanced signal. The fact that all microwave systems are connected by either waveguide or coaxial cable presents us with the need for a frequency independent, or at least a quasi-frequency independent, device which will convert the signal on the transmission line to one which is balanced. Such a device is known commonly as a balun. Two baluns are investigated in this thesis, one of which is based on a reflection coefficient approach and the other on a gradual change in the mode of propagation on the transmission line.

CHAPTER II

THEORY OF LOGARITHMICALLY PERIODIC ANTENNAS.

2.1 Evolution of the Log- Periodic Dipole Array:

The notion of an antenna defined entirely by angles as being frequency independent was first introduced by V.H. Rumsey some twenty years ago. Since the antenna had to be defined by angles, the first logical step in antenna design was the so-called equi-angular spiral antenna illustrated in figure 2.1. The equations describing the generation of the pattern for the arms of this antenna are given by the equi-angular or logarithmic spiral equations:

$$r = \exp (a(\theta - \delta)) \quad (2.1.1)$$

$$\text{or equivalently } \theta - \delta = \frac{1}{a} \ln (r) \quad (2.1.2)$$

where the variables r and θ are conventional polar coordinates.

The equations which trace out the arms of the antenna are:

$$r_1 = K \exp (a\theta) \quad (2.1.3)$$

$$r_2 = K \exp (a(\theta - \delta)) \quad (2.1.4)$$

for one arm, and:

$$r_3 = K \exp (a(\theta - \pi)) \quad (2.1.5)$$

$$r_4 = K \exp (a(\theta - \pi - \delta)) \quad (2.1.6)$$

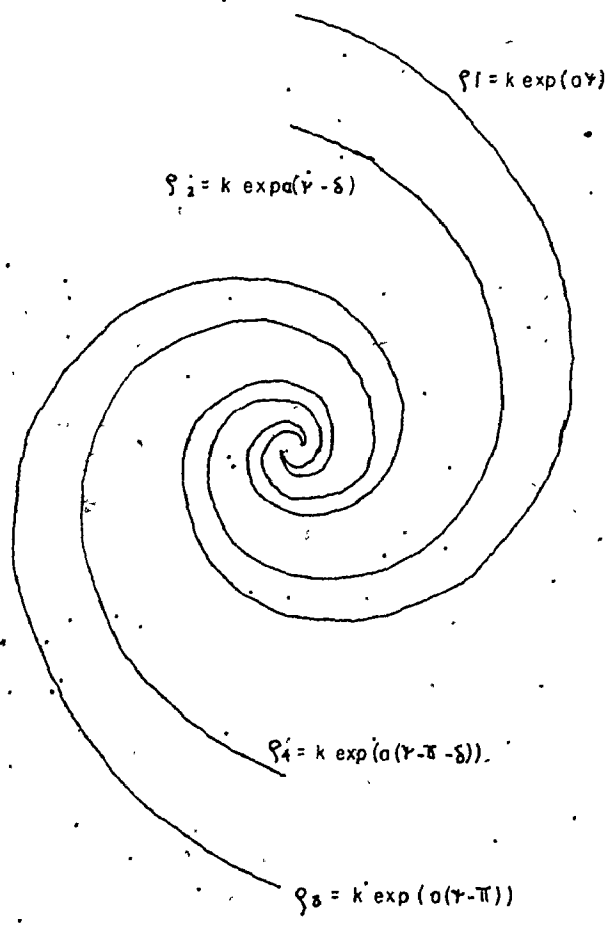


FIGURE 2.1

EQUI-ANGULAR SPIRAL ANTENNA

The constants 'a' determine the tightness of the spiral, K the size of the terminal region and δ the width of each arm.

The antenna is excited by a balanced source at the centre terminals with the current flowing along the spiral arms until a region is encountered where the spacing between arms is of the order of half a wavelength. The energy is radiated from this region with little or, ideally, no energy travelling further along the arms. It is important to note here that there are three distinct regions on the antenna which, as will be seen, are necessary for the proper operation of a frequency independent antenna. These are (i) the transmission region which simply acts as a transmission line for the incident energy to feed (ii) the active region which is that part of the device which actually radiates the energy and (iii) the reflective region which acts to attenuate any energy which has leaked past the active region. It is also of great importance to observe that the active region moves along the arms of the antenna with frequency in order to maintain a constant radiating aperture in terms of wavelengths. This phenomenon of scaling ensures that the antenna is frequency independent, and is fundamental to the successful operation of any frequency independent device.

With the success of the equiangular spiral antenna, Duhamel proposed that it was possible to radiate energy from structures which, besides being described in terms of angles, had some properly situated disturbances along its length (5). Such a device was the planar log-periodic antenna shown in figure 2.2.

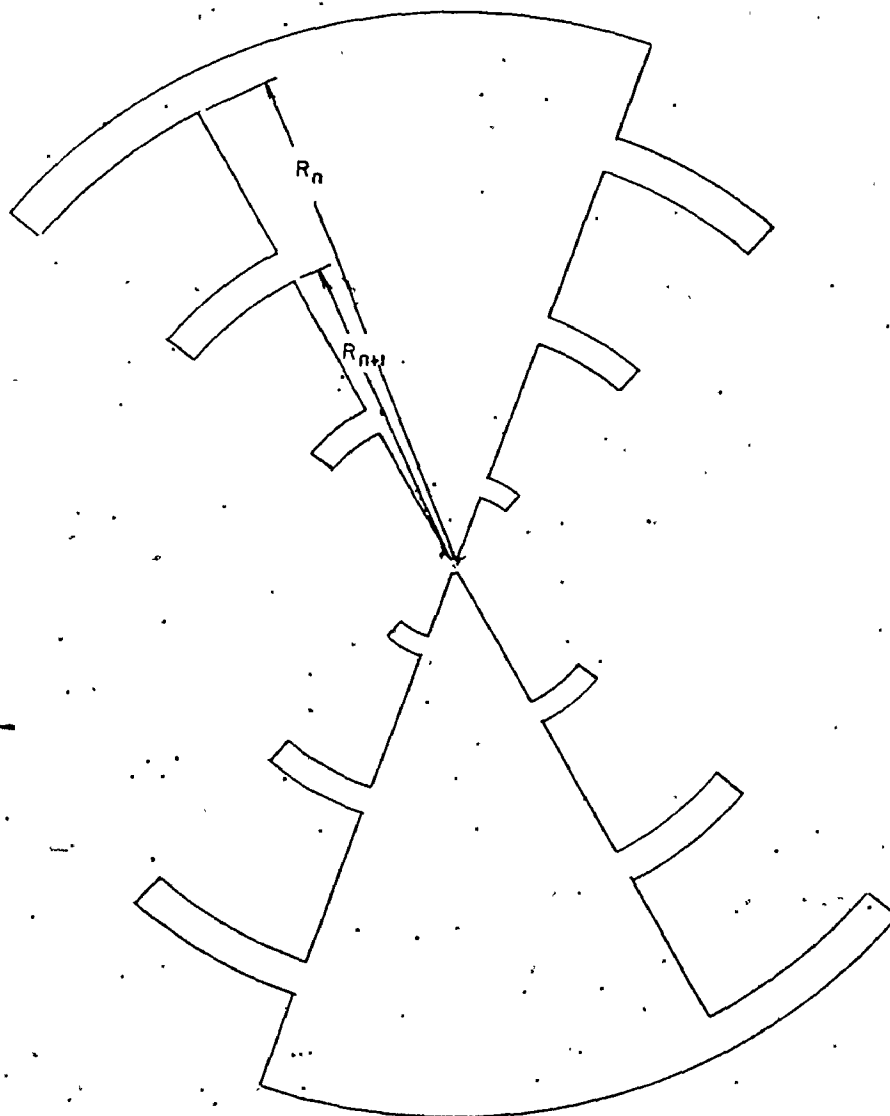


FIGURE 2.2

PLANAR LOG - PERIODIC ANTENNA.

The log-periodic structure is essentially two planes of metal having teeth cut into them at radii, R_n , with the spacing between radii defined by a constant ratio:

$$\tau = \frac{R_{n+1}}{R_n} \quad (2.1.7)$$

The spacing ratio, τ , not only defines the distance between successive teeth, but also the ratio of successive lengths and widths of teeth.

$$\begin{aligned} \tau &= \frac{R_{n+1}}{R_n} \\ &= \frac{W_{n+1}}{W_n} \\ &= \frac{L_{n+1}}{L_n} \end{aligned} \quad (2.1.8)$$

It is clearly the case that for an infinite structure, the properties which apply at any frequency f will also apply at multiples of the fundamental

$$f, \tau f, \tau^2 f, \dots, \tau^n f$$

As a result it can be seen that any such property which may occur at frequency f (impedance, pattern, polarization) will reappear at frequencies which are periodic with the logarithm of the spacing

factor, τ , thus giving the name "logarithmically-" or "log-" periodic. Although the log-periodic antenna is not truly frequency independent but periodic, the variation of antenna characteristics does not change significantly for values of $0.8 \leq \tau < 1.0$.

As was the case with the planar equiangular spiral antenna, the planar log-periodic antenna exhibited a bi-directional radiation pattern extending equally from both sides of the antenna plane. In order to obtain a more unidirectional characteristic, Isbell folded the arms of the device toward each other to form a V - shaped geometry. The results of this action were two fold. Firstly, as was expected, the radiation pattern became unidirectional although it was in the backward direction instead of forward as was originally hypothesized. Secondly, although the input impedance of the antenna remained constant as a function of frequency, the value of the impedance was found to vary as a function of the angle between the arms of the antenna.

With the success of the non-planar log-periodic antenna, it was very tempting to allow the arms to fold together until the subtended angle became zero and to replace the teeth with monopole elements. The resulting structure would remain log-periodic but would be much simpler than the non-planar log-periodic in the respects that (i) the array is again confined to a single plane and (ii) the curved teeth are replaced by simple dipoles.

The resulting structure, as the previous description would imply, was labelled the log-periodic dipole array (henceforth known

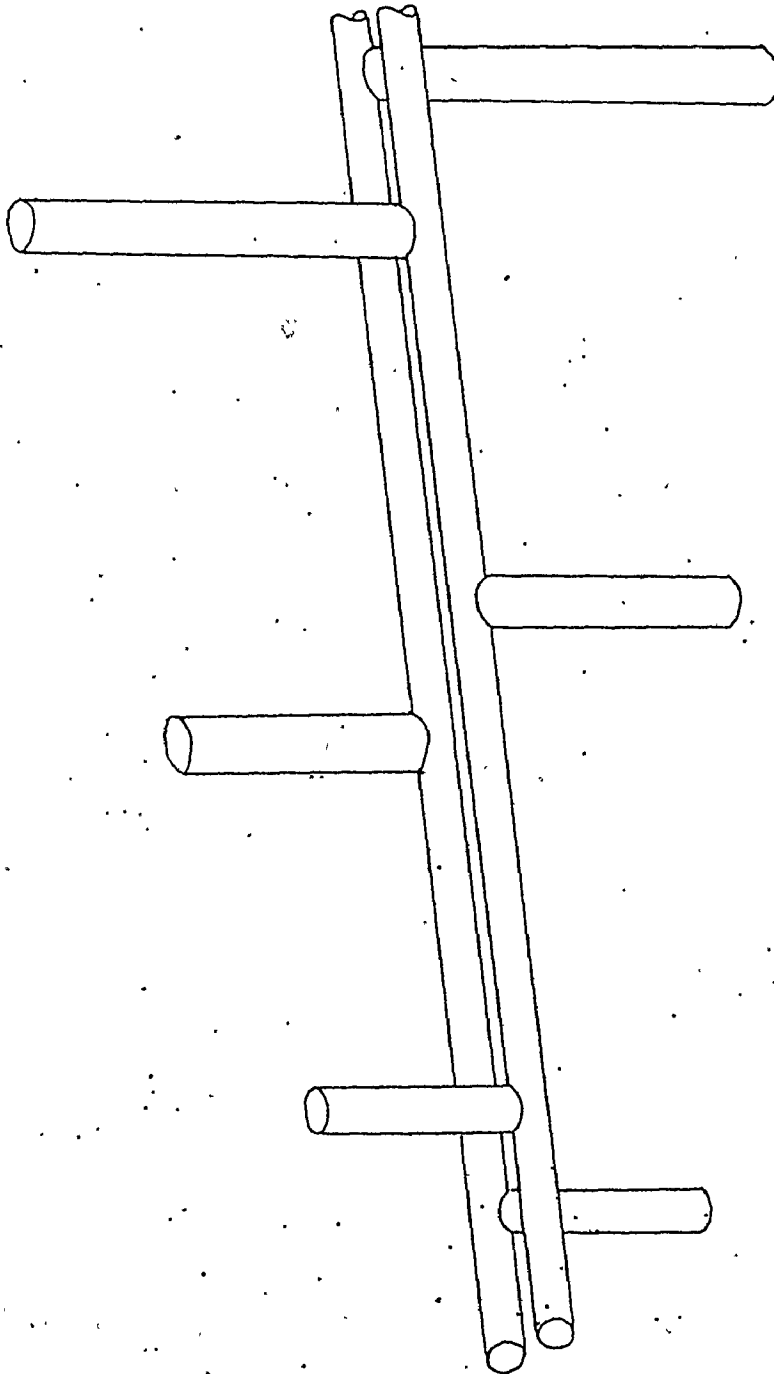


FIGURE 2 3

LOG - PERIODIC DIPOLE ARRAY.

as the LPDA), and is shown in figure 2.3.

2.2 LPDA Theory of Operation:

Before dealing with the fundamental principles on which the log-periodic dipole array operation is based, it will be useful, in further discussion, to make reference to the parameters which describe the geometry of the array.

The physical dimensions of the LPDA are shown in figure 2.4. Note that there are three parameters which completely describe the array configuration, those being:

- (1) τ ; the scaling constant which determines the length of each successive element. The scaling constant is defined by:

$$\tau = \frac{R_{n+1}}{R_n} \quad (2.2.1a)$$

$$= \frac{h_{n+1}}{h_n} \quad (2.2.1b)$$

h_n = half length of the n^{th} dipole

R_n = distance from virtual apex, P, to the n^{th} element.

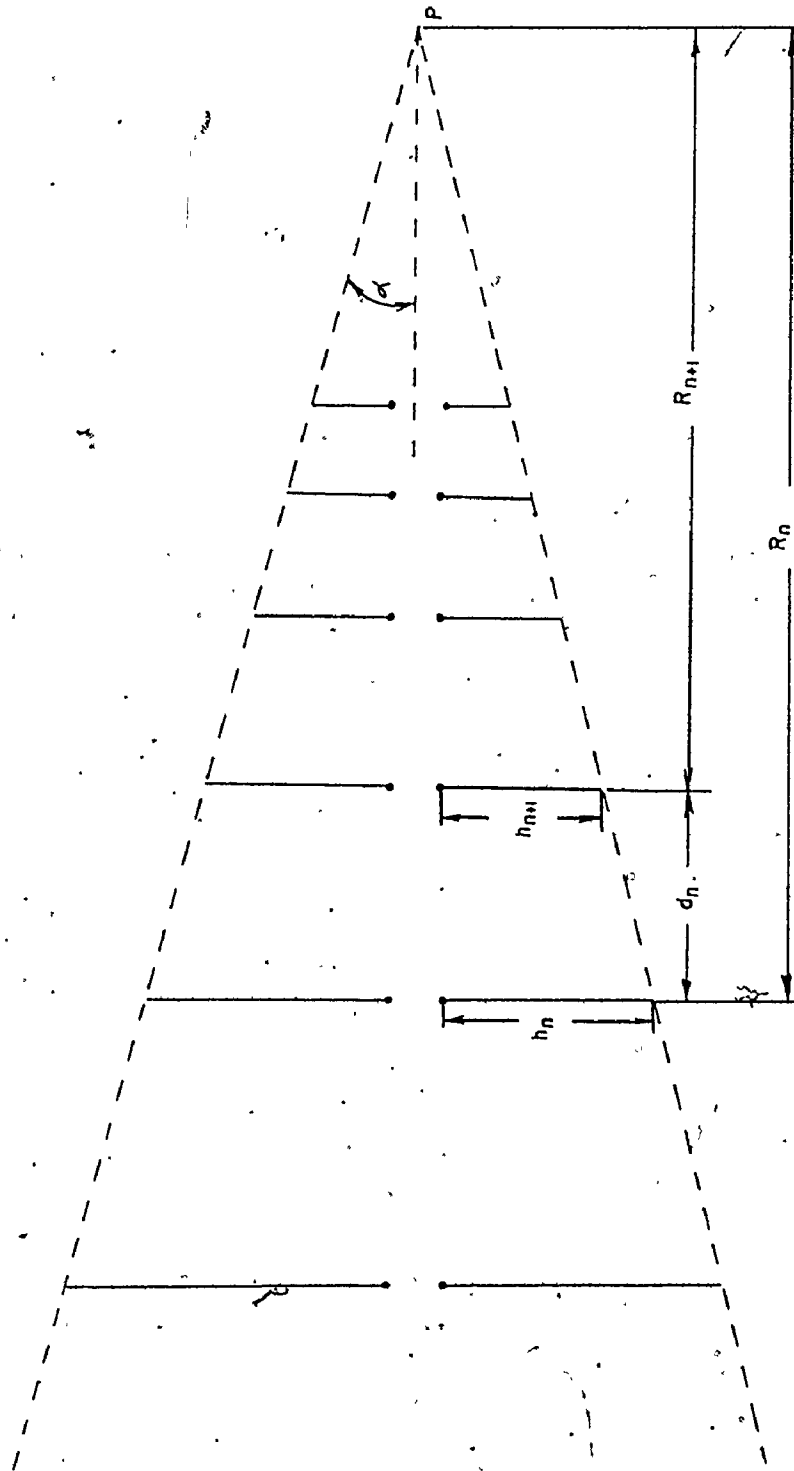


FIGURE 2 4

LPDA GEOMETRY.

(ii) σ ; the spacing constant which is the distance in wavelengths between successive dipole elements. The spacing constant is defined by:

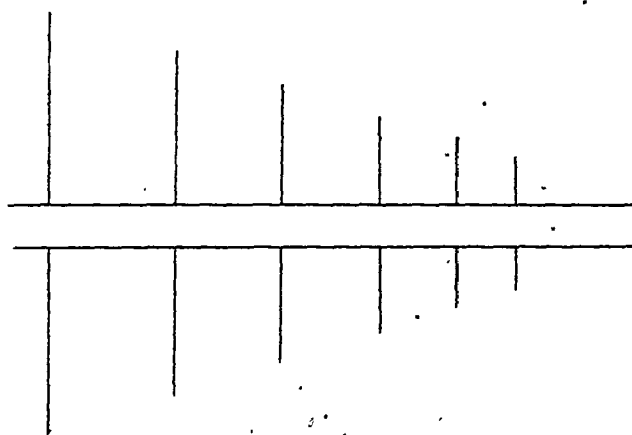
$$\sigma = \frac{d_n}{4h_n} \quad (2.2.2)$$

where d_n is the physical distance separating element n from element $n+1$

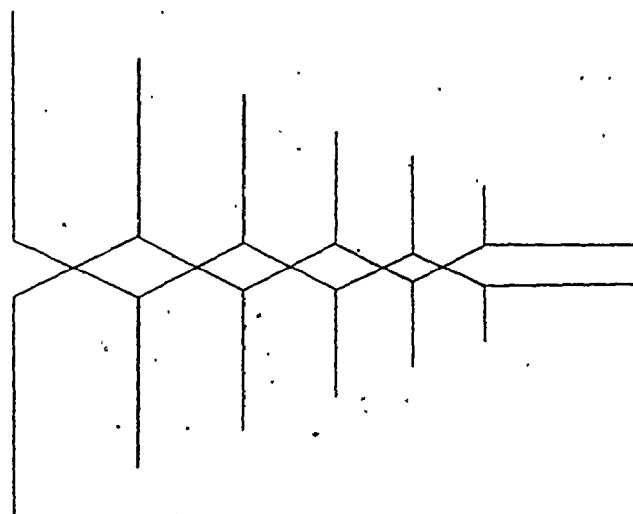
(iii) α ; the half angle of the array subtended by the ends of the dipole elements from virtual apex, P . The half angle is given by:

$$\alpha = \tan^{-1} \frac{h_n}{R_n} \quad (2.2.3)$$

The initial method for feeding the dipoles was to have an ordinary transmission line connecting the dipoles together thus causing the phase progression along the array to be in the forward direction, i.e. toward the larger dipoles. It was immediately discovered, however, that the larger elements caused sufficient interference to break up the beam emitted from the active region. So that in order to prevent interference by the long elements in the beam path, it was reasoned that instead of allowing the phase progression to be in the forward direction, it should be in the backward direction where the small elements would have relatively little effect on the pattern. The method



(a)



(b)

FIGURE 2.5

UNSUCCESSFUL (a) & SUCCESSFUL FEEDS FOR LPDA.

by which this was achieved was by alternating the phase of each successive element by 180° as shown in figure 2.5. By doing this two ends were achieved: (i) the phase progression in the active region was such that radiation was in the backward direction forcing the main beam off the apex of the array and (ii) relatively short and closely spaced (in wavelengths) front elements would have nearly opposite phasings and thereby contribute little to the overall radiated field.

It is interesting to note that the necessity for opposite element phasing was not immediately realized from observation of the geometry of the non-planar log-periodic antenna. It is clearly the case that the teeth are arranged asymmetrically along the two sections of transmission line formed by the arms of the array, thus automatically invoking the alternate phasing requirement.

It would appear initially that the analysis of log-periodic dipole operation would be a tremendous task because of the variable lengths, spacings and values of current on the elements comprising the array. In fact this is the case if one maintains that an exact analysis is to be performed since the concepts used to describe uniform arrays no longer hold true. A good approximation to the behaviour of the array can be made by considering it to be a locally periodic structure whose period varies slowly as a function of distance from virtual apex, P (6). Now, one can see that if a wave is launched on the structure and encounters the active region, this wave, if the active region is properly designed, will be radiated in the backward

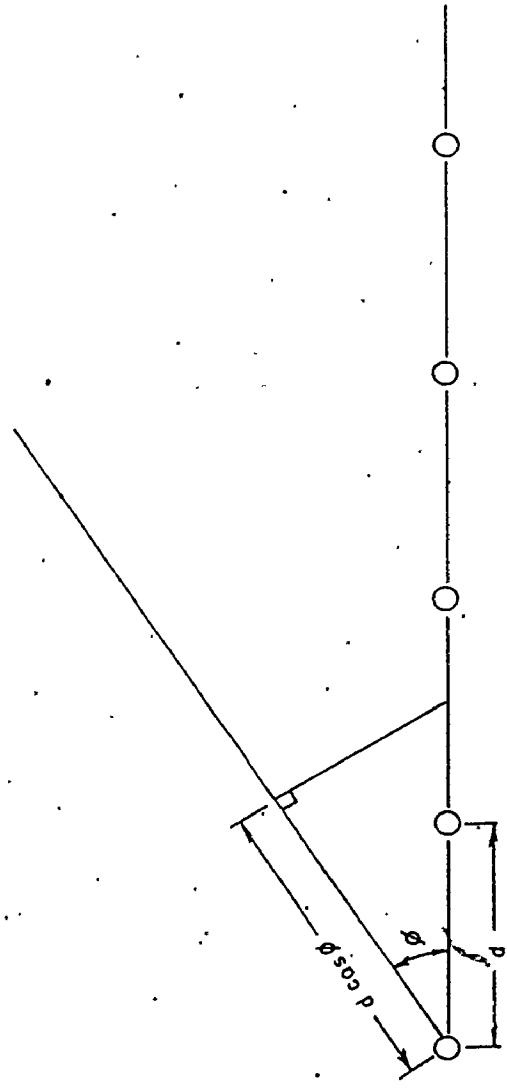


FIGURE 2 6
LINE ARRAY OF ISOTROPIC SOURCES.

direction by the resonant elements, the radiation pattern being approximately that of a uniform array having approximately the same period as the active region. The analysis of at least the radiation pattern may now be carried out using conventional uniform array theory.

If one considers an array of N equally spaced isotropic radiators (see figure 2.6), then the magnitude of the radiated field is given by

$$|E| = 1 + \left| \sum_{n=1}^{N-1} \exp(jn\psi) \right| \quad (2.2.4)$$

where $\psi = Kd \cos \phi + \alpha$

α = progressive phase shift, left to right,
along the array

d = element to element spacing

The letter K is used here to symbolize the free space phase shift constant, $K = 2\pi/\lambda_0 = \omega/c$ as opposed to the symbol β , the phase shift constant of the array itself $\beta = 2\pi/\lambda = \omega/v$, ' v ' being the phase velocity of a wave propagating along the array. It is easy to show that the magnitude of the electric field is a maximum for $\psi=0$, so that for source spacings smaller than a half wavelength, the angle of maximum radiation is given by

$$\phi_{\max} = \cos^{-1} \frac{-\alpha}{Kd} \quad (2.2.5)$$

Clearly, for no progressive phase shift, $\alpha=0$ and $\phi_{\max}=\pm 90^\circ$; i.e. a two lobed broadside pattern. With a lagging phase shift $-Kd < \alpha < 0$, the lobes tilt toward the front of the array with increasing phase lag until the condition $\alpha = -Kd$ is met in which case a unidirectional lobe extending from the front of the array is formed. Similarly, with a phase lead $0 < \alpha < Kd$, the broadside lobes tilt toward the back of the structure until $\alpha = +Kd$ and radiation is maximum endfire in the backward direction.

Observe also that for $|\alpha| \gg Kd$, the phasor summation in equation 2.2.4 becomes very small regardless of ϕ giving a rather weak field distribution in all directions with no major lobe.

Using the results obtained from equations 2.2.4 and 2.2.5, one may proceed in the description of log-periodic behaviour. Remember also, that in feeding the dipoles the transmission line is crossed over between successive elements giving an inherent leading phase progression of 180° .

Consider first the transmission region. Here, the elements are rather short in terms of wavelengths and consequently supply a fair amount of capacitance to the transmission line. The current in each element is small and leads the transmission line voltage by about 90° . Also, since the dipoles are spaced closely together, in wavelengths, the adjacent elements are close to, but somewhat less than, 180° out of phase. This anti-phase condition combined with the closeness of the elements suggest that the field, if any is generated at all, will be weak and in the backfire direction.

Having passed through the transmission region with relatively little attenuation, the signal will encounter an active region where the dipoles are close to being a half wavelength long. Since these elements are the primary radiators in the array, their impedance has a dominant resistive component due to the radiation resistance of the elements. As a result, the element currents are close to being in phase with the base voltage having a slight lag below and slight lead above the resonant frequency. Also, the spacing between elements has increased in terms of wavelengths so that the phase progression is leading by an angle $\alpha = \pi - \beta d = \pi/2$ radians. This condition satisfies the requirement necessary to produce the strong backfire lobe which is desired in log-periodic design.

Although it is desired that the active region extract and radiate all of the incident energy, this is not entirely true in practice, as some small percentage of the incident wave is transmitted through. Thus it becomes important to have a third region beyond the active region which will rapidly attenuate any signal which leaks through. If one considers the LPDA to be a periodically loaded transmission line, as shown in figure 2.7, it is clear that the longer elements behind the active region present an inductive reactance to the energy filtering through. At some point in this region, the shunt inductance will dominate over the transmission line capacitance and the energy encounters the attenuation region of a distributed element low pass filter.

In this attenuation region, the phase shift per unit length

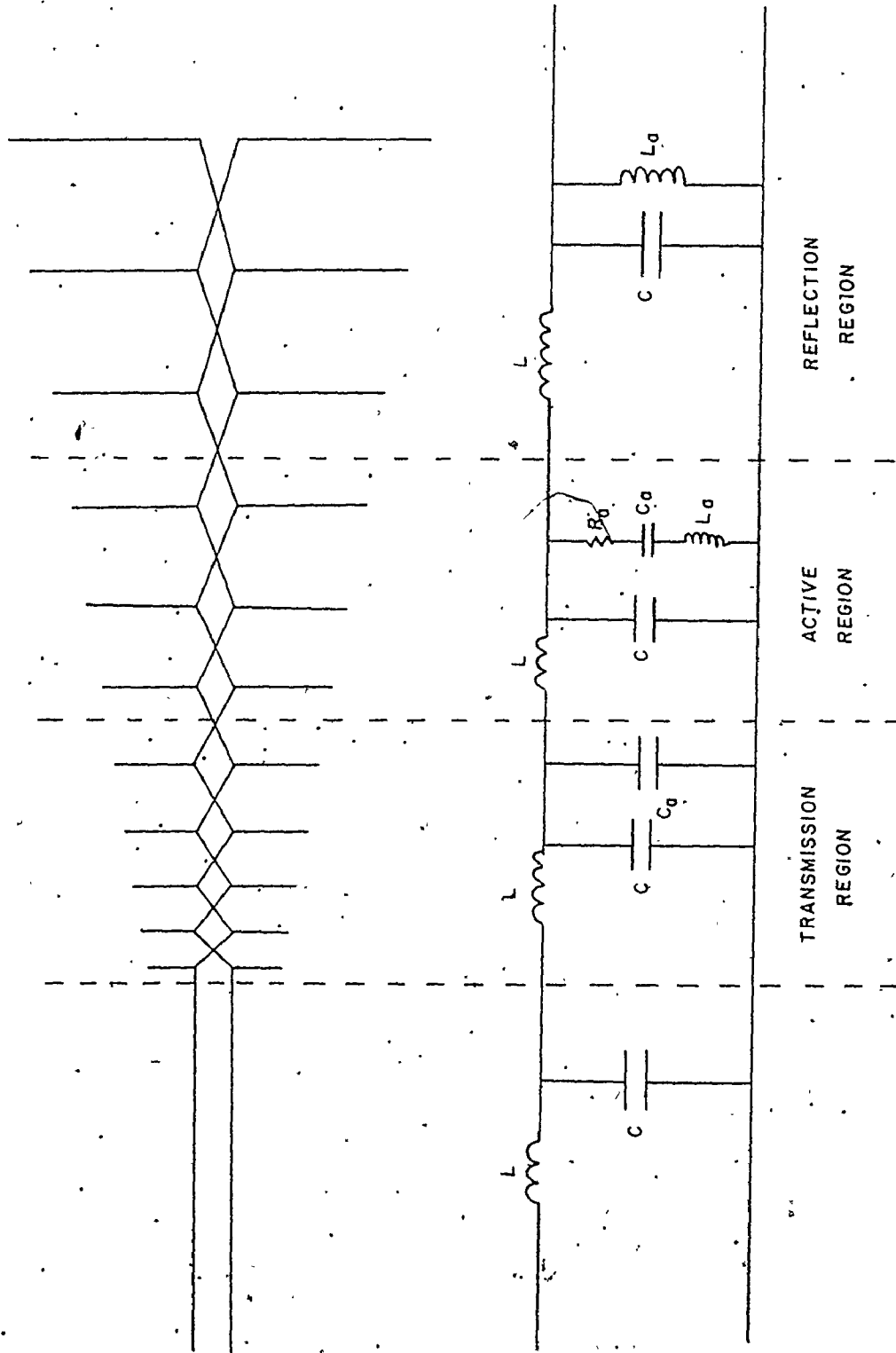


FIGURE 2.7

/ TRANSMISSION LINE MODEL FOR THE LPDA.

on the transmission line is ideally zero in the lossless case and the phase velocity becomes infinite which implies no wave motion in the forward direction. Now since the wave is inhibited from moving forward and there are no radiating elements, the only alternative is for the energy to be reflected back toward the active region. Illustration of the action in the three regions was given by Carrel (3) the results of which are shown in figure 2.8.

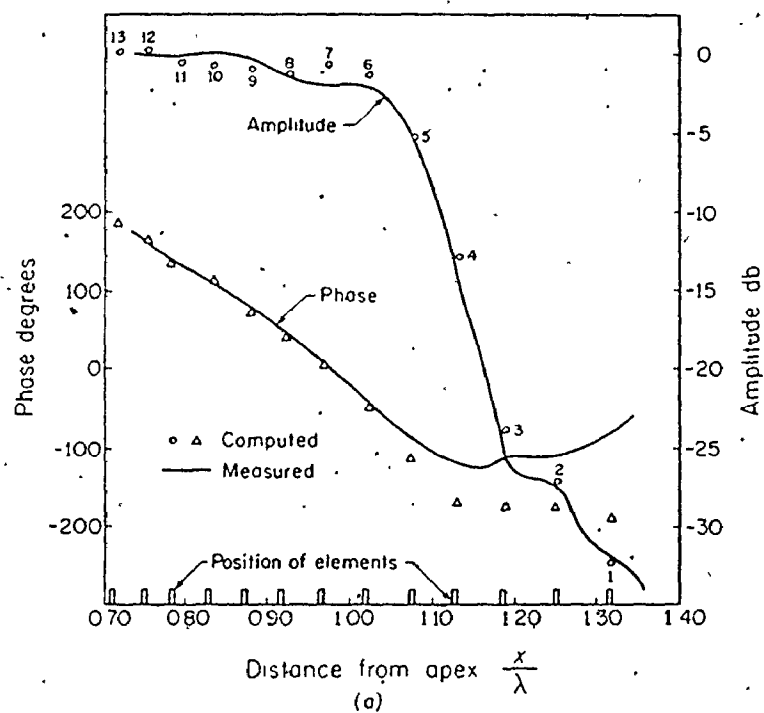
2.3 LPDA Design Procedure:

The main theme in designing a microwave printed circuit LPDA does not vary appreciably from the method outlined by Carrel (3) although corrections must be made in calculating the input impedance and the directivity must be determined by experimental observation:

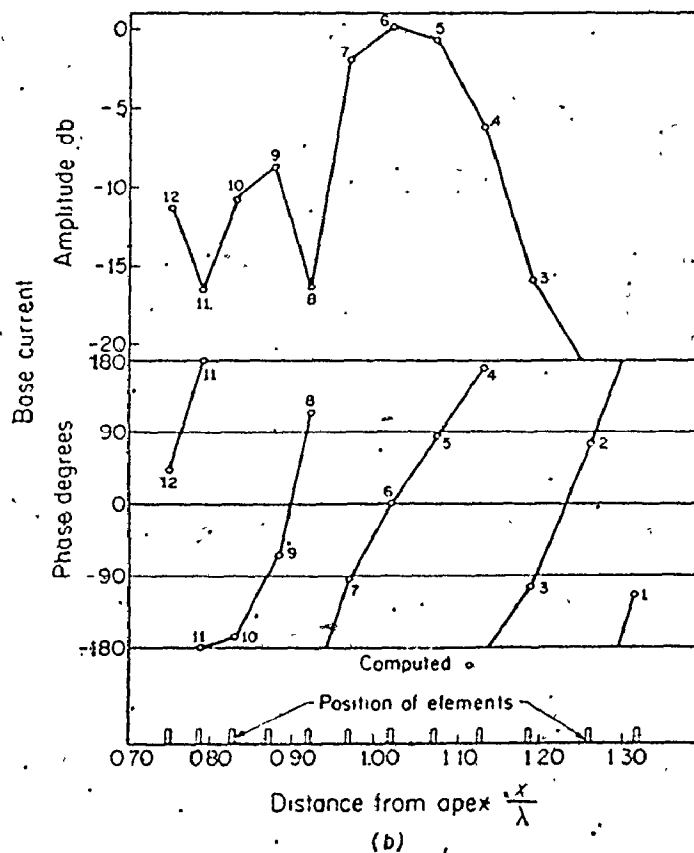
It is also important to note here that some practical limitation on the parameters τ , σ , and α needs to be made. Through past experience, it has been found that the scaling factor, τ , should be kept in the range

$$.81 \leq \tau \leq .95$$

For values larger than 0.95, the array tends to become very long and if the scaling constant is smaller than 0.81, the number of elements in the array for a given bandwidth becomes small. This forces the active region to be limited to a very small number of elements, perhaps even just a single element. The amount of energy which passes through the active region to the reflection region then becomes



TRANSMISSION LINE VOLTAGE



ELEMENT CURRENTS

FIGURE 2.8

VOLTAGES & CURRENTS ALONG LPDA (after Carrel (3))

appreciable reflecting a substantial amount of energy back toward the terminals of the array thereby destroying the log-periodic nature of the device. The structure half angle, being related to the scaling constant also has limitations imposed on it such that

$$20^\circ \leq \alpha \leq 40^\circ$$

For those values of half angle greater than 40° , the elements become too closely spaced to accurately maintain the proper element to element spacing and, corresponding to large values of scaling constant, values of half angle smaller than 20° force the array to become too long to be of any practical use.

The spacing constant, σ , is also given a useful range such that

$$.05 \leq \sigma \leq \sigma_{\text{opt}}$$

For values of spacing constant smaller than 0.05 the array directivity falls off quite rapidly and the input impedance varies with frequency (3). The upper bound on the spacing constant, σ_{opt} , is the so-called optimum value for σ . It was found by Carrel (3) that for a given value of scaling constant, τ , the optimum spacing constant would give a maximum directivity and a minimum input voltage standing wave ratio. Values of spacing constant greater than the optimum value have a tendency to introduce sidelobes in the radiation pattern.

In the design procedure outlined by Carrel, it was suggested that one choose the desired directivity and input impedance of the array and from these constraints, choose the values of scaling and spacing constants which give these characteristics from previously determined graphs. The situation here is not quite so simple as the array is supported in an inhomogeneous medium and the charts which were developed by Carrel no longer apply. The fact that the dipoles in the array are on a dielectric would lead one to speculate that the near field surrounding the immediate neighbourhood of the array would be distorted in some manner or another from its free space distribution, thus giving rise to a distortion in the far field. Since the extent to which the dielectric affects the near field is not readily known, it is left merely to observe the far field pattern and draw some tentative conclusions from it. An all-encompassing chart of directivity and input impedance as a function of τ and σ for an array in the presence of a dielectric can be made but is beyond the scope of this thesis and is not dealt with here. For the purposes of the work presented here, τ and σ were chosen for convenience and ease of construction of the array and the input impedance and directivity observed and compared with the values which one might expect from a similar device in free space.

Another variation from Carrel's work arises in the fact that the dipole elements themselves are no longer cylindrical but are planar instead. One can no longer use the results for the characteristic impedance of a dipole because of the different geometry and

also the fact that the dipoles are loaded capacitively by the dielectric. Again, the dipole impedance as a function of height to width ratio, h/w , can easily be determined experimentally.

The effect of the dielectric substrate increasing the capacitance of a dipole introduces the notion that the resonant frequency of the dipole would decrease from its free space value.

Recall that for a wave travelling in free space, its velocity is given by

$$f_o \cdot \lambda = c \quad (2.3.1)$$

where c = speed of light in vacuo

Now if radiation of the same wavelength propagates through some medium having relative dielectric permittivity ϵ_r , then the frequency is reduced from its free space value according to

$$f_d \cdot \lambda = \frac{c}{\sqrt{\epsilon_r}} \quad (2.3.2)$$

or, by simultaneous solution of equations 2.3.1 and 2.3.2;

$$f_d = \frac{f_o}{\sqrt{\epsilon_r}} \quad (2.3.3)$$

Now if one considers a dipole to be the source of radiation in a dielectric, the wavelength of the propagating energy remains the same because of the aperture of the dipole but the frequency is

reduced as

$$f_{rd} = \frac{f_{ro}}{\sqrt{\epsilon_r}} \quad (2.3.4)$$

f_{rd} = resonant frequency of dipole in dielectric

f_{ro} = resonant frequency of dipole in free space

Thus by making a trial measurement of the resonance point of a dipole on a dielectric, one can determine how large the effective dielectric constant, ϵ_{eff} , is and use it toward any design having the same basic geometry.

As was mentioned before the value of the spacing constant has a specific value which is optimum in the sense of providing maximum directivity and minimum S.W.R. for a given value of scaling constant. Through the graphs provided by Carrel in his paper (3), an empirical formula for σ_{opt} has been proposed (9, 17) and is given as

$$\sigma_{opt} = 0.258 \cdot \tau - 0.066 \quad (2.3.5)$$

Once having chosen the desired values for scaling and spacing constants, the structure half angle is calculated as

$$\alpha = \tan^{-1} \frac{(1-\tau)}{4\sigma} \quad (2.3.6)$$

The bandwidth is calculated as

$$B = \frac{f_{\text{lower}}}{f_{\text{upper}}} \quad (2.3.7)$$

If it were the case that the active region consisted of only one dipole, then the bandwidth of the actual structure, B_s , would approach the design bandwidth, B . However, as has been discussed in section 2.2, the active region usually includes more than one element and, consequently, is wider than might be expected. Because the active region contains more than one element, the performance of the antenna array may start to deteriorate as the active region begins to include the longest or shortest elements. It is for this reason that the structure bandwidth must be made larger than the desired bandwidth by some factor, B_{ar} , the bandwidth of the active region.

$$B_s = B \times B_{ar} \quad (2.3.8)$$

Since the boundary between the active region and the transmission and reflection regions is often not clearly defined, B_{ar} cannot be given a clear-cut value. To circumvent this problem an empirical expression for B_{ar} has been proposed (7)

$$B_{ar} = 1.1 + 7.675(1-\tau)^2 \cot \alpha \quad (2.3.9)$$

Having found the bandwidth of the active region, the structure bandwidth may be found from equation 2.3.8. The number of elements required in the array is given by

$$N = 1 - \frac{\log B_s}{\log \tau} \quad (2.3.10)$$

Clearly, the number of elements in an array must be an integer and that N , in general, is not integer. To overcome this, one merely takes the next integer number greater than N simultaneously increasing the bandwidth of the structure slightly due to the addition of an extra element.

Finally, the spacing between elements is found to be

$$d_n = 4\sigma h_n \quad (2.3.11)$$

If desired, one can also calculate the overall length of the structure before construction. This can be found by using

$$L = \frac{\lambda_{\max}}{4\sqrt{\epsilon_{\text{eff}}}} \left(1 - \frac{1}{\epsilon_s} \right) \cot \alpha \quad (2.3.12)$$

In the course of the design, it may be found that the structure length or some other parameter does not satisfy the design specifications. As a result, it would be necessary to alter

the values for τ , σ , and α and repeat the design until specifications are met. This iterative process is simplified to some extent through the aid of the nomograms reproduced from Carrel (3) and shown in figures 2.9, 2.10 and 2.11.

2.4 Terminal Impedance of the LPDA:

Well designed log - periodic antennas often exhibit standing wave ratios of 1.5:1 or better, even with very abrupt front truncation so long as a well formed active region remains on the structure. By considering the LPDA as the transmission line structure described in section 2.2, one can formulate a very accurate approximation to the input impedance of the structure. This transmission line analysis was first presented by Carrel (3) and is followed rather closely here with the necessary modifications added for the effects due to the dielectric substrate.

Using the loaded transmission line concept, one can see that in the transmission region, the relatively short dipoles add a shunt capacitance, proportional to their length, periodically along the line. The spacing between elements does not change and therefore the capacitance per unit length of transmission line is constant. Herein lies the justification of adding a single valued lumped capacitance to the characteristic capacitance of the transmission line. The impedance of a dipole is given as

$$Z = -jZ_a \cot \beta h \quad (2.4.1)$$

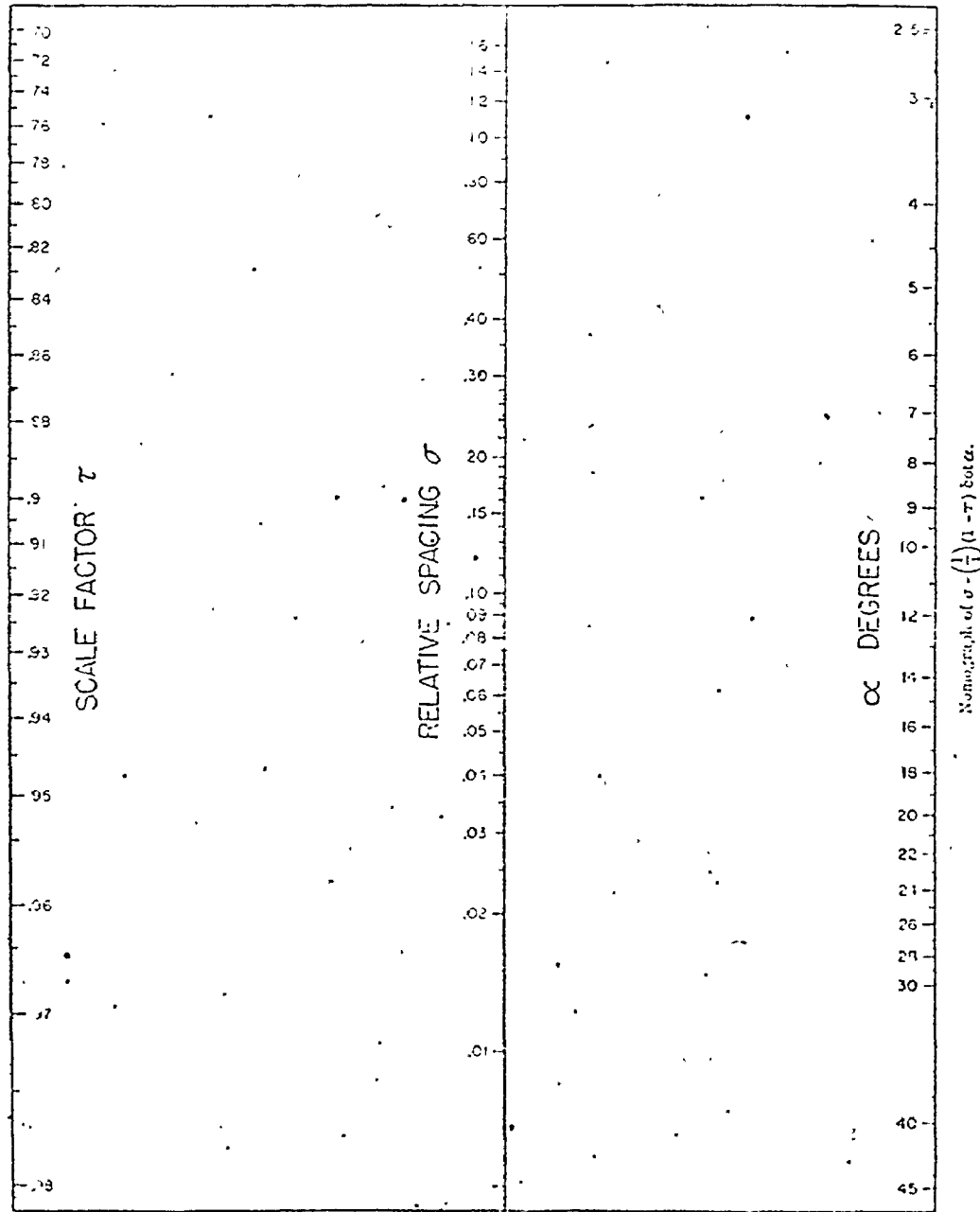


FIGURE 2.9

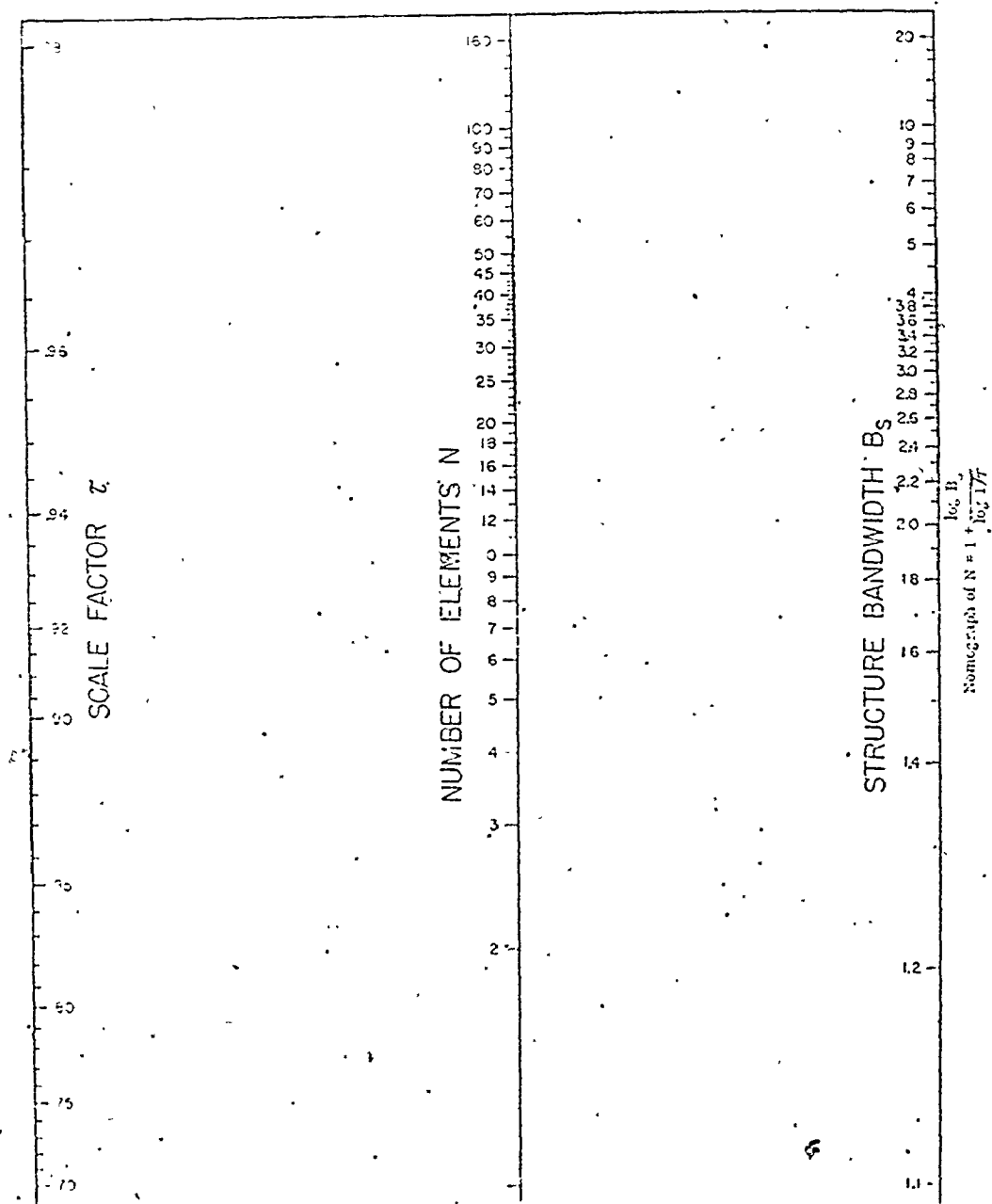


FIGURE 2.10

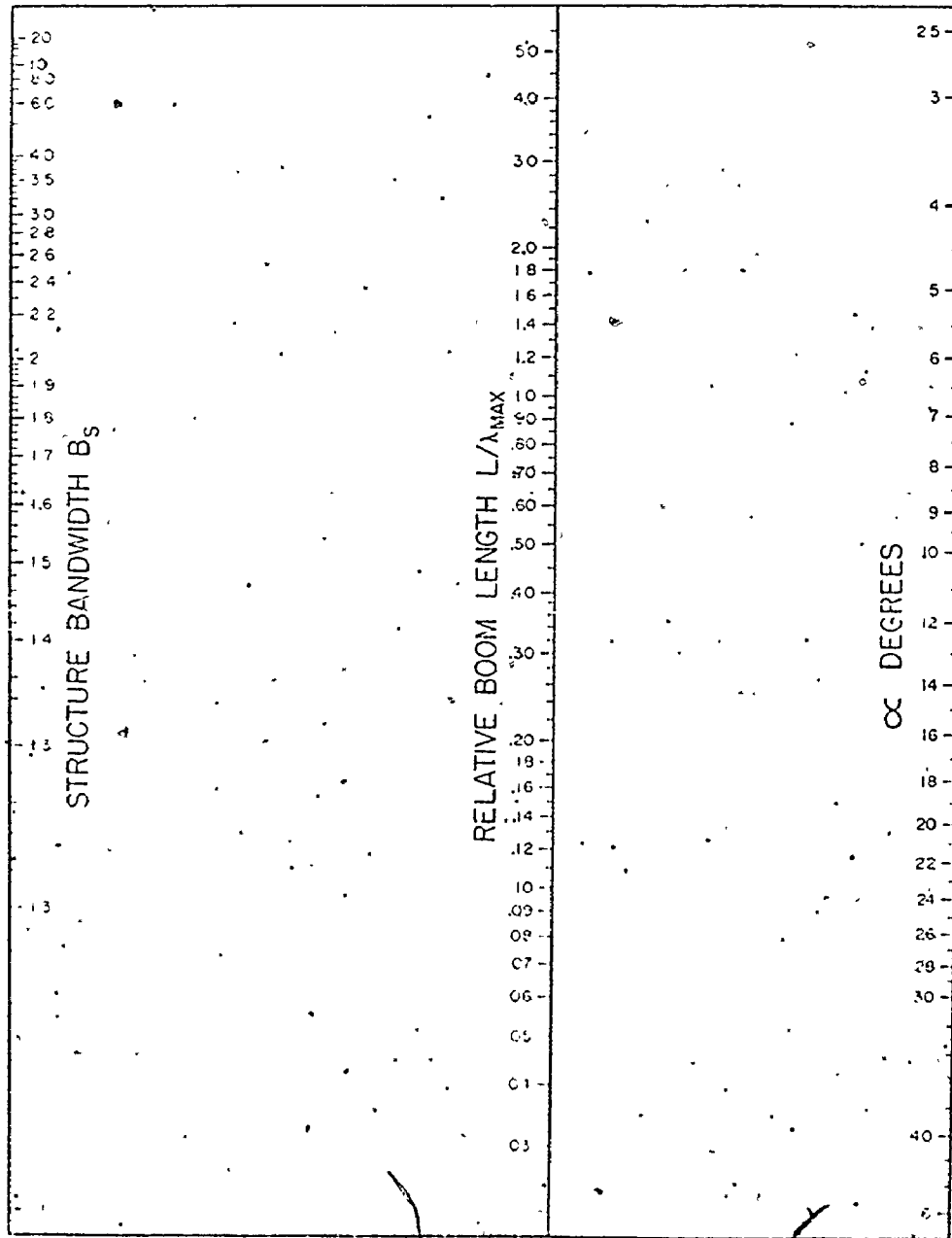


FIGURE 2.11

By replacing the cotangent function with its small argument equivalent, one can postulate the capacitance of a particular dipole element to be

$$C_n = \frac{h_n}{v_p Z_a} \quad (2.4.2)$$

v_p = phase velocity in the presence of a dielectric

$$\frac{c}{\sqrt{\epsilon_r}} \leq v_p \leq c$$

If one considers a worst case condition in equation 2.4.2, namely that the dipoles are completely enveloped by a dielectric then one can initially place upper and lower bounds on the dipole capacitance between that in free space and that when totally surrounded by dielectric.

$$\frac{h_n}{Z_a} \leq C_n \leq \frac{h_n \sqrt{\epsilon_r}}{Z_a} \quad (2.4.3)$$

Through experimental measurement, one can establish empirically what the effective dielectric constant is and proceed in a more accurate calculation of input impedance. In the present derivation, however, calculations will be made assuming the dipoles are completely surrounded by dielectric in order to arrive at some bounding values for the feeder impedance.

If one considers a mean spacing, d_{mean} , at dipole 'n' defined by

$$d_{\text{mean}} = \sqrt{d_n d_{n-1}} \quad (2.4.4)$$

then the average capacitance per unit length of transmission line is

$$\begin{aligned} \Delta C &= \frac{C_n}{L} \\ &= \frac{h_n \sqrt{\tau \epsilon_r}}{c d_n^2 a} \end{aligned} \quad (2.4.5)$$

But recall from equation 2.3.11 that the spacing factor is $\sigma = 4d_n/h_n$. Thus equation 2.4.5 becomes

$$\Delta C = \frac{\sqrt{\tau \epsilon_r}}{4\sigma^2 a} \quad (2.4.6)$$

Recall also the fundamental relationships

$$Z_o = \sqrt{\frac{L_o}{C_o}} ; \quad c = \frac{1}{\sqrt{L_o C_o}} \quad (2.4.7)$$

Using equation 2.4.7, one can now formulate an approximate expression for the impedance of the loaded transmission line.

$$R_o = \sqrt{\frac{L_o}{C_o + \Delta C}} \quad (2.4.8)$$

substituting $R_o = \sqrt{\frac{L_o}{C_o + \frac{\sqrt{\epsilon_r}}{4cZ_a\sigma}}}$ (2.4.9)

or $R_o = \frac{Z_o}{\sqrt{1 + \frac{\sqrt{\epsilon_r}}{4\sigma} \frac{Z_o}{Z_a}}}$ (2.4.10)

The feeder impedance, Z_o , can now be easily found through inversion of equation 2.4.10 to give

$$Z_o = \frac{R_o^2 \sqrt{\epsilon_r}}{8\sigma' Z_a} + R_o \sqrt{\left(\frac{R_o \sqrt{\epsilon_r}}{8\sigma' Z_a}\right)^2 + 1} \quad (2.4.11)$$

$$\sigma' = \frac{\sigma}{\sqrt{\epsilon_r}}$$

Thus one now has bounding values for Z_o between which some particular value of relative dielectric permittivity will give the best match.

$$\frac{R_o^2}{8\sigma' Z_a} + R_o \sqrt{\left(\frac{R_o}{8\sigma' Z_a}\right)^2 + 1} \leq Z_o \leq \frac{R_o^2 \sqrt{\epsilon_r}}{8\sigma' Z_a} + R_o \sqrt{\left(\frac{R_o \sqrt{\epsilon_r}}{8\sigma' Z_a}\right)^2 + 1} \quad (2.4.12)$$

2.5 Summary:

To summarize the steps involved in designing a log-periodic dipole array, a step by step procedure is outlined here to aid in the practical design of an array.

- (i) Make a trial measurement on a dielectrically supported dipole to determine its average characteristic impedance as a function of height to width ratio and also measure the effective dielectric constant of the medium.
- (ii) Establish the desired bandwidth B and input impedance R_0 .
- (iii) Choose a convenient set of values for the scaling and spacing factor to give reasonable dimensions of the array.
- (iv) Calculate the structure half-angle from equation 2.3.6
- (v) Calculate the bandwidth of the active region from eq. 2.3.9
- (vi) Calculate the structure bandwidth from equation 2.3.8
- (vii) Calculate the number of elements from equation 2.3.10
and the length of the longest element $L_1 = \frac{\lambda_{\max}}{4\sqrt{\epsilon_{\text{eff}}}}$
- (viii) Having found the length of the first element, determine its width from the desired impedance level found in (i).
- (ix) Knowing the dimensions of the longest element, calculate the spacing to the next element from equation 2.3.11 and the dimensions of the next element
$$L_{n-1} = L_n \times \tau; W_{n-1} = L_{n-1} \times \frac{h}{w}$$
- (x) Finally calculate the required impedance for the transmission line feeding the array elements from eq. 2.4.12

In the designs presented here, the antennas were etched from a dielectric board necessitating the use of photolithography in order to properly sensitize the sections which were to be etched away and mask the areas where copper was to remain. To simplify making the mask, a computer program written in FORTRAN IV is supplied in Appendix A which calculates the dimensions of the LPDA required and also returns cutting coordinates for making the mask. A detailed account of the photolithographic procedure is also outlined in Appendix B.

CHAPTER III

FEED MECHANISMS FOR THE LPDA.

3.1 Necessity for a Balun:

Normally one may consider that all that is involved in designing an antenna system is the actual building of the antenna itself and then simply attaching it to the cable running from the transmitter or receiver. In most applications concerning radiation and especially above V.H.F. such action could lead to disastrous results.

If one attempts to make an analysis of a transmission line, one may find that a potentially infinite number of modes of propagation may exist and must be taken into account. However if one makes the assumption that the higher ordered modes are sufficiently attenuated, the analysis may be simplified by including only the dominant lower ordered modes (8).

Consider the coaxial line shown in figure 3.1. Normally if the coaxial line is connected to a generator that is electrically shielded, then only the balanced mode of propagation is launched and no current flows on the outside of the shield because of the lack of any external electric field. Observe, however, the consequences of attaching the end of the line to a simple dipole antenna as in figure 3.2 (10). Since the balanced currents I_1 and I_2 are equal in magnitude, it is seen that the current flowing in the element connected to the outside conductor must be smaller than I_2 due to the branching.

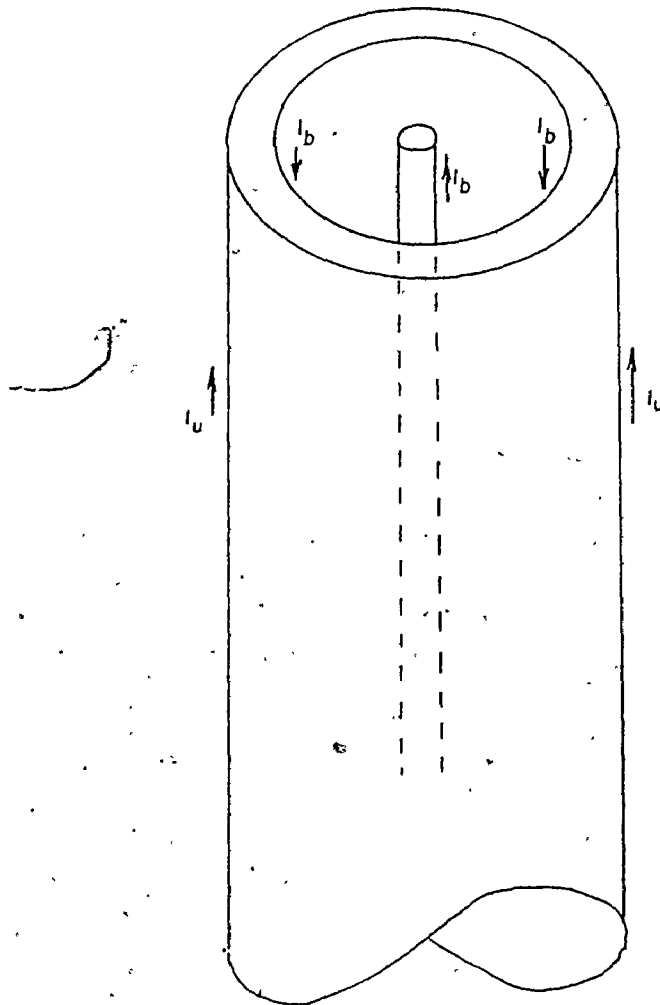


FIGURE 3.1.

BALANCED & UNBALANCED MODES ON COAXIAL LINE.

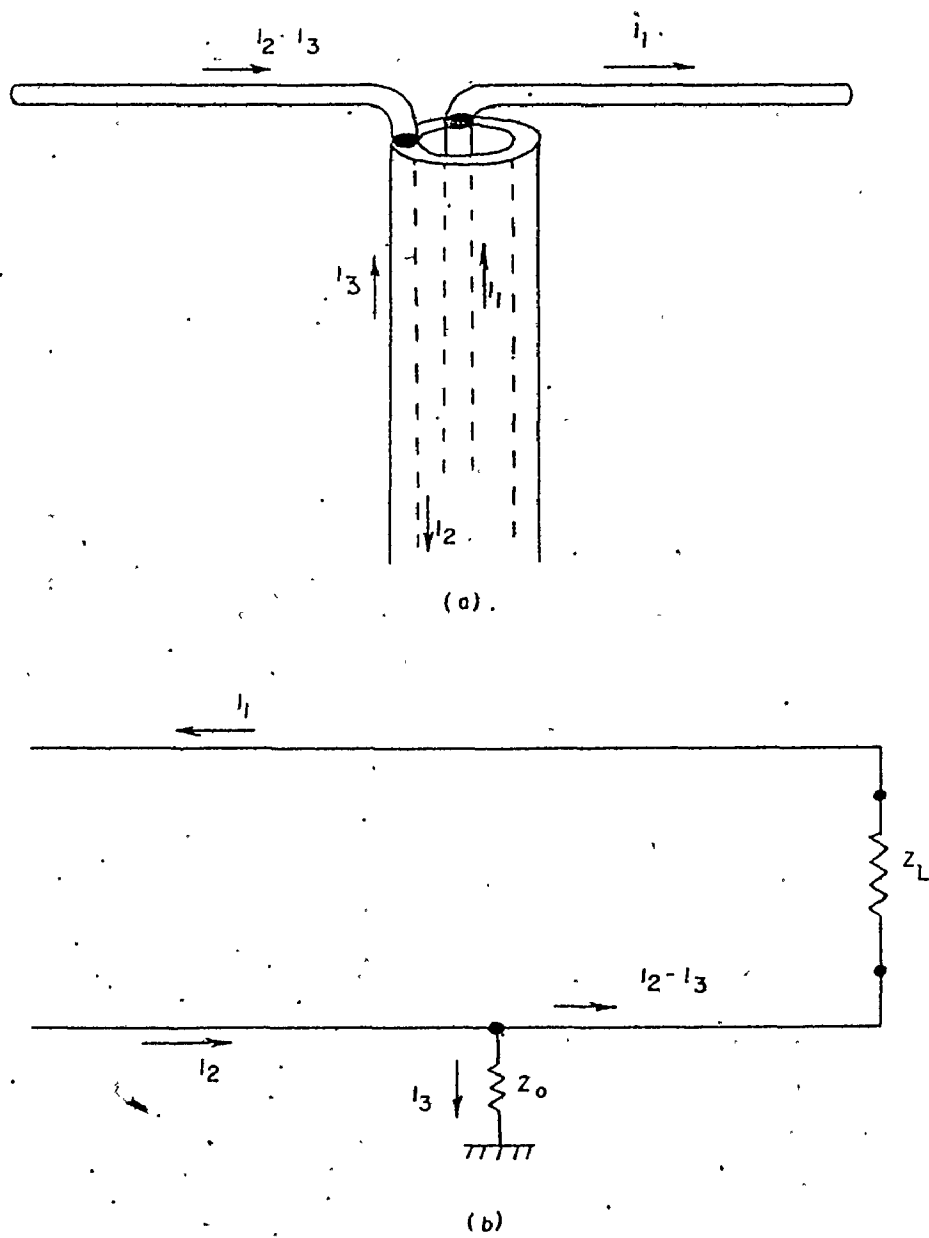



FIGURE 3.2
EFFECT OF DIRECTLY ATTACHING A DIPOLE TO COAXIAL LINE
AND EQUIVALENT CIRCUIT.

of I_2 between the radiating element and the shield. Two consequences arise from this branching of I_2 . Firstly, the currents flowing in the dipole are not equal in magnitude giving rise to a deviation in the normal radiated field one might expect from a dipole. This unbalance in the currents gives us the term "unbalanced mode" and note also that this unbalanced mode is excited only when the proper conditions exist at the terminals of the cable. Secondly and perhaps more important, one observes that the shield now has a current I_3 flowing on it. This current, whether in the transmitting or receiving case, is associated with an electric field extending between the outside conductor and earth. Thus, since I_2 and I_3 both combine to form the return path to the generator for I_1 , the entire length of the cable acts as an antenna and, depending on the magnitude of I_3 may or may not dominate the radiation pattern emitted by the dipole. It is obvious, then, that the direct connection of a dipole or array of dipoles to a coaxial line will give results that probably will not resemble dipole operation at all. The "trick" to successfully feeding a dipole is then to suppress current I_3 as much as possible or, more desirably, avoid generating I_3 in the first place. Numerous successful methods have been devised to provide such a "balanced feed", the most commonly known of which is the balun transformer.

3.2 Frequency Independent Baluns:

As was just stated in the previous section, many baluns have



been invented based on a variety of concepts including transformer coupling (9,11), splitting the incident energy and shifting the phase in one branch (18), and transmission line matching (10, 11). However, it is the case that none of the above mentioned methods of obtaining a balanced feed are truly frequency independent. Some can be made fairly broadband as in the transformer coupling method whereas some, such as the phase shifting method, are fairly sharply tuned to one particular frequency.

Only a small fraction of all baluns have been found to be truly frequency independent. These are the self-balun (2), which has been used to successfully feed many free space log-periodic arrays, and the mode converter (8, 12).

The self-balun, shown in figure 3.3, is a rather elegant method of feeding a balanced load in that instead of preventing the unbalanced current I_3 from flowing on the outside of the shielded cable, it is allowed to flow until it reaches a radiating region where it naturally becomes the balanced current I_2 . The fact that such an arrangement can be used with a log periodic dipole array arises from the presence of the active region. Since the active region extracts and radiates most of the incident energy, there is a rapid decline in current along the antenna elements and, consequently, the transmission line behind the active region. This lack of current flowing on the transmission line give rise to a substantially field free region behind the active region and the unbalanced current is not generated.

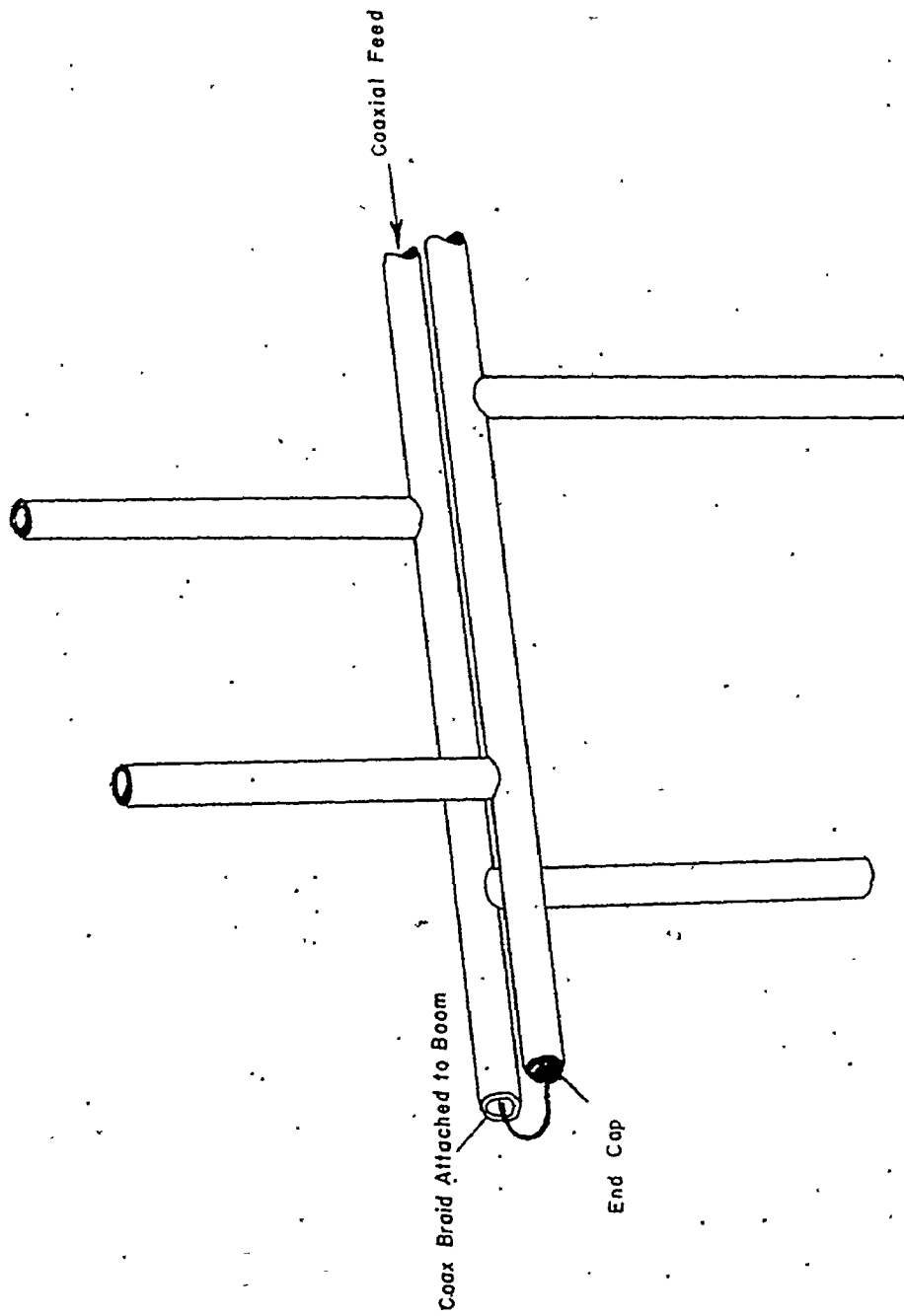
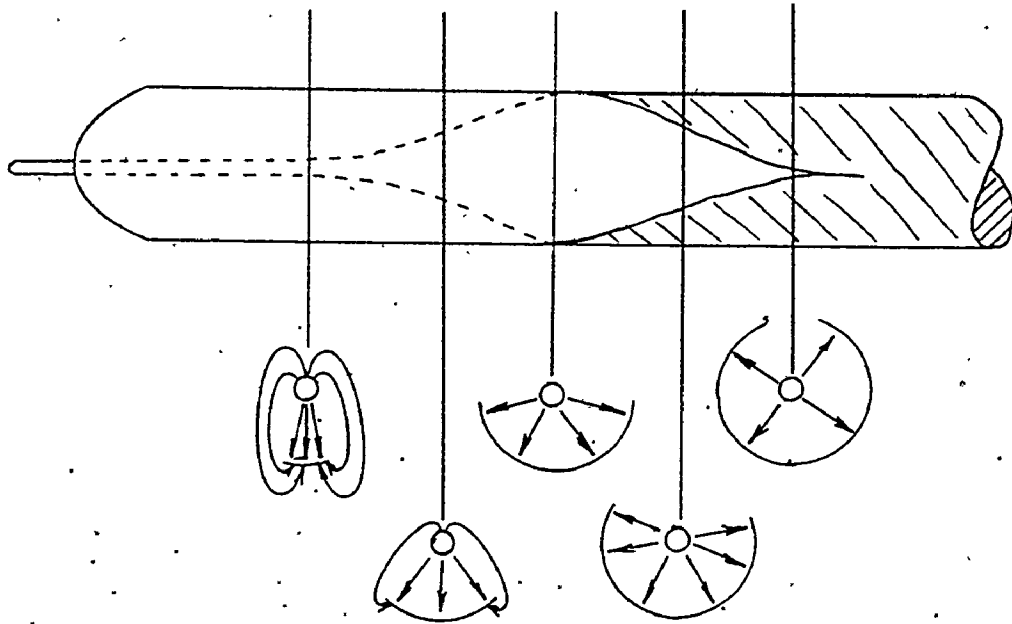


FIGURE 3 3

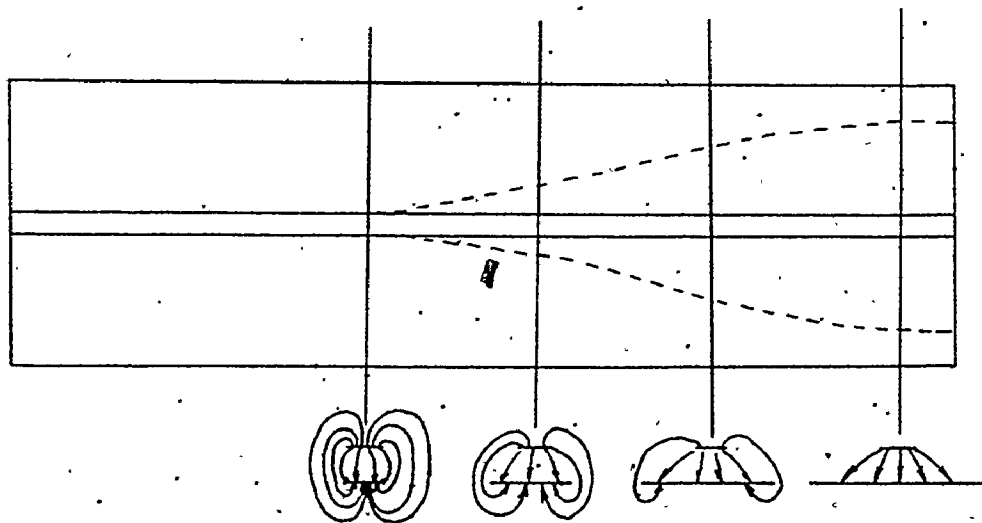
SELF-BALUN METHOD FOR FEEDING LPDA.

The second device operates on the principle of making a gradual transition from a coaxial conductor geometry to that of twin lead. The structure is shown in figure 3.4 illustrating both the original idea presented by Duncan & Minerva (12) and its extension to a stripline geometry as given by Rumsey (8). The transition along the length of the structure performs, as the name implies, a conversion from a semi-TEM wave at the input to a full TEM wave at the output which is characteristic of a balanced two conductor transmission line. This device, although not truly frequency independent, can be broadbanded to any arbitrary degree by spreading the transition out to a sufficient number of wavelengths and can also be used as an impedance converter between the coax and device if the two characteristic impedances are not the same. This transformation of impedance is done through the implementation of an optimum Dolph - Chebyshev taper along the length of the device (13).

A third type of balun structure, based on a reflection coefficient principle is proposed here (23). The device, shown in figure 3.5 consists of two layers of dielectric supporting one half of the antenna array, the centre conductor for a shielded strip-line and the remaining half of the antenna respectively. At the antenna feed point, one half of the array is short circuited to the centre conductor whereas the other half is left open forming an arrangement similar to that of the self-balun. The operation of this device is different from the self-balun, however, in that use is made of the reflection coefficients at the terminal region of the antenna



(a) (after (12))



(b). (after (8))

FIGURE 3.4

COAXIAL (a) & MICROSTRIP (b) MODE CONVERTERS.

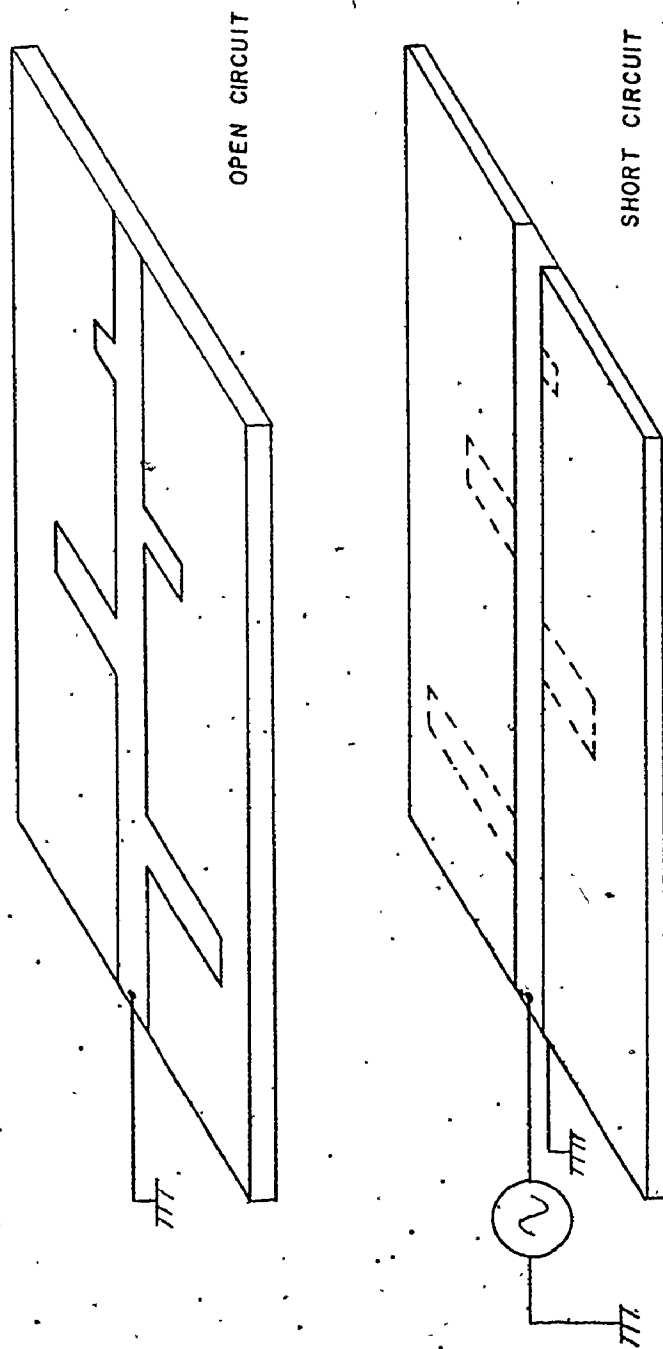


FIGURE 3.5
REFLECTION BALUN GEOMETRY.

feed point to cancel any reflected voltage on the centre conductor, and, at the same time, provide a balanced voltage across the transmission line feeding the antenna.

In figure 3.5, the incident field is imagined to be a superposition of two electric field vectors, one directed toward the upper shield and the other toward the lower shield. Upon reaching the end of the structure, the electric fields experience reflection coefficients of $\rho = +1$ at the open termination and $\rho = -1$ at the short circuited termination. If one assigns some arbitrary value, V , to the incident voltage, then the reflected voltages would be $+V$ at the open circuit and $-V$ at the short circuit. The resulting effect would be that a balanced voltage is produced across the shield, which eventually is the transmission line for the antenna, and a net of zero volts on the centre conductor.

CHAPTER IV

DESIGN AND PERFORMANCE OF AN M.P.C. LOG-PERIODIC DIPOLE ARRAY

4.1 General:

The material used in fabricating the antennas here was Rexolite #1422 microwave laminate printed circuit board. This material is made of fairly low loss dielectric having a relative dielectric constant of $\epsilon_r = 2.54$ and thickness of 0.794 mm. The quoted dielectric constant is guaranteed to 10 GHz, making it conducive to microwave fabrication and the small thickness of the board is helpful in keeping the terminal separation of the dipoles to a minimum. Antenna characteristics were measured in an R.F. anechoic chamber at the Communications Research Laboratory with the aid of a Hewlett-Packard automatic network analyser.

4.2 Determination of Dipole Impedance and Extent of Dielectric Loading:

As stated in Chapter 2; it is necessary to first determine the average characteristic impedance of a dielectrically supported dipole before design of an LPDA can begin.

The easiest way to determine this was to fabricate such a dipole, shown in figure 4.1, and measure its S_{11} (input return loss) parameter by means of the network analyser. The dipole itself, as can be seen in the photograph, is excited from a mode converter described in section 3.2. The reason for using the mode converter here

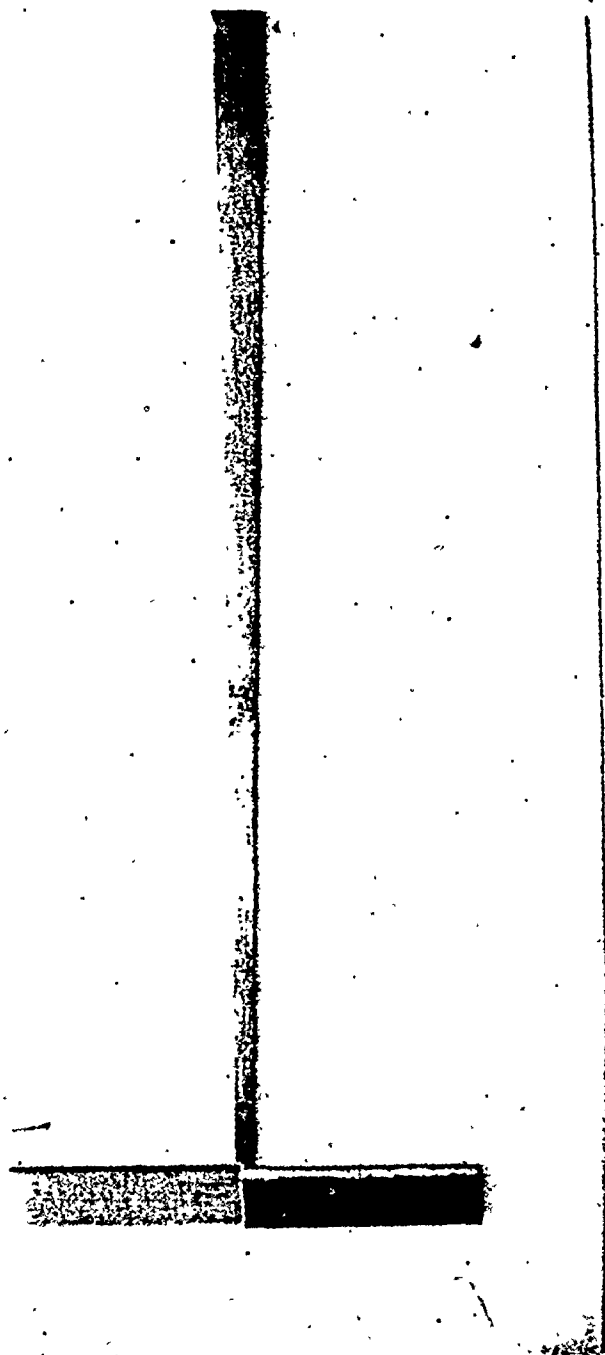


FIGURE 4 I

HALF WAVE DIPOLE FED FROM MODE CONVERTER.

was twofold: (a) since the impedance of the dipole is unknown and remains to be found, the mode converter could be made to have a constant impedance of 50Ω along its length to match with the attendant coaxial cable and still measure the return loss from the dipole; (b) since it is also desired to measure the extent of dielectric loading on the dipole, the frequency independent nature of the converter would facilitate measurement of return loss and frequency shift simultaneously. The design of the mode converter follows:

Required input impedance: 50 ohms

Required output impedance: 50 ohms

Lowest frequency to be passed: 2.0 GHz.

Since the input of the mode converter is microstrip, one might think that a fairly large ground plane is needed to obtain the required input impedance as all calculations to this end are made on the assumption of the presence of an infinite ground plane. Such is not the case, however; it has been found (15) that ground planes of the order of three conductor widths are sufficient to contain the electric field in the desired region and thus maintain the impedance quite close to the theoretical value.

The calculation of structure dimensions are easily found from the design charts given in Appendix C.

Dielectric constant = $2.54 \times \epsilon_0$

Coaxial line impedance = 50 ohms

Conductor width to separation ratio (μ strip) = 2.9

(from fig. C-1)

Conductor width = 2.30 mm.

Ground plane width = 6.9 mm.

Balanced line width to separation ratio = 3.75

(from fig. C-3)

Conductor width = 2.98 mm.

The length of the converter could be obtained from following the procedure in (13) but, as one can immediately see, the fact that no change of impedance is involved gives a trivial solution of no taper over any arbitrary length. In other words the transmission line continues to infinity having infinitely little taper. Since we want to taper the ground plane to form a balanced line, it is sufficient to taper the ground plane over a distance longer than a half wavelength at the minimum desired frequency in the pass band.

$$L > \frac{3 \times 10^{10}}{2 \times 10^9 \times 2}$$

$$= 7.5 \text{ cm.}$$

For ease of construction and assurance that a sufficiently smooth taper was provided, the converter was made 12.5 cm. long in this particular case.

Impedance measurements were made by time domain reflectometry and results are shown in figure 4.2. Notice that in figure 4.2a the impedance of the mode converter tends to decrease near the centre of the device. This is most likely due to the fact that at this particular point along the structure, the electric field configuration is such that the transmission line is behaving more like a balanced stripline rather than a microstrip. If this is the case, then one may reason that the characteristic capacitance of the transmission line is much greater than that capacitance giving an impedance of 50 ohms. The capacitance must therefore be decreased to maintain a constant impedance along the structure. This was done by trimming the width of the microstrip conductor until a constant fifty ohm impedance was observed on the T.D.R. (figure 4.2b).

The average characteristic impedance of the dipole was determined from swept frequency measurements of S_{11} shown in figure 4.3. By observing the magnitude of the return loss, one can determine the reflection coefficient and, hence the magnitude of the dipole characteristic impedance, Z_a .

$$|\rho| = \text{antilog} (-\text{Return loss} / 20) \quad (4.2.1)$$

$$|Z_a| = Z_0 (1+\rho/1-\rho) \quad (4.2.2)$$

The values for Z_a as a function of dipole half height to width ratio are presented in table 4.2.1 and plotted in figure 4.4.

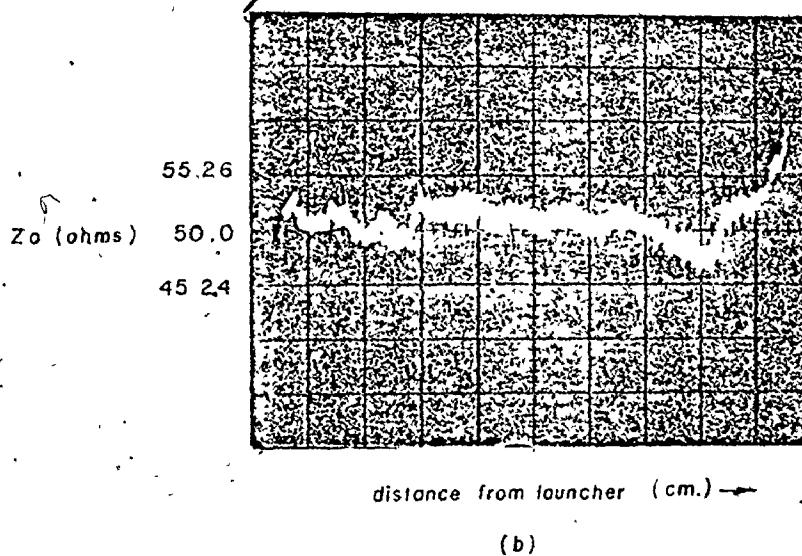
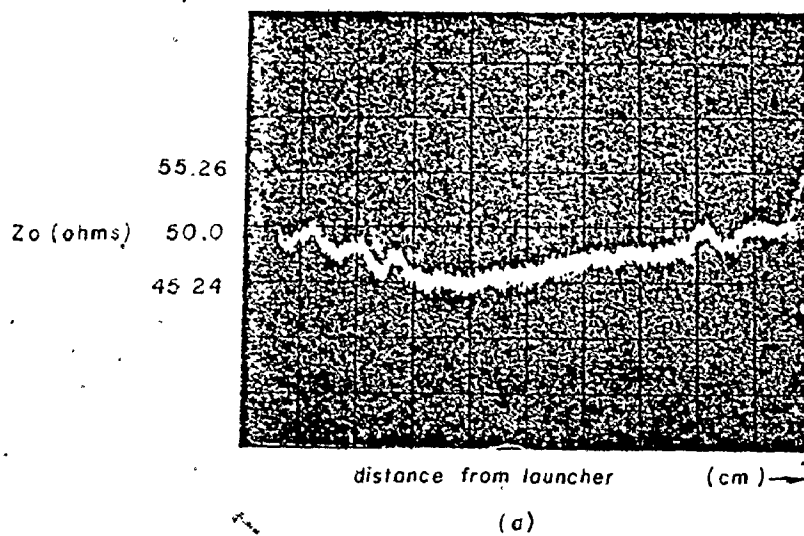


FIGURE 4.2

MODE CONVERTER BEFORE (a) & AFTER (b) COMPENSATION.

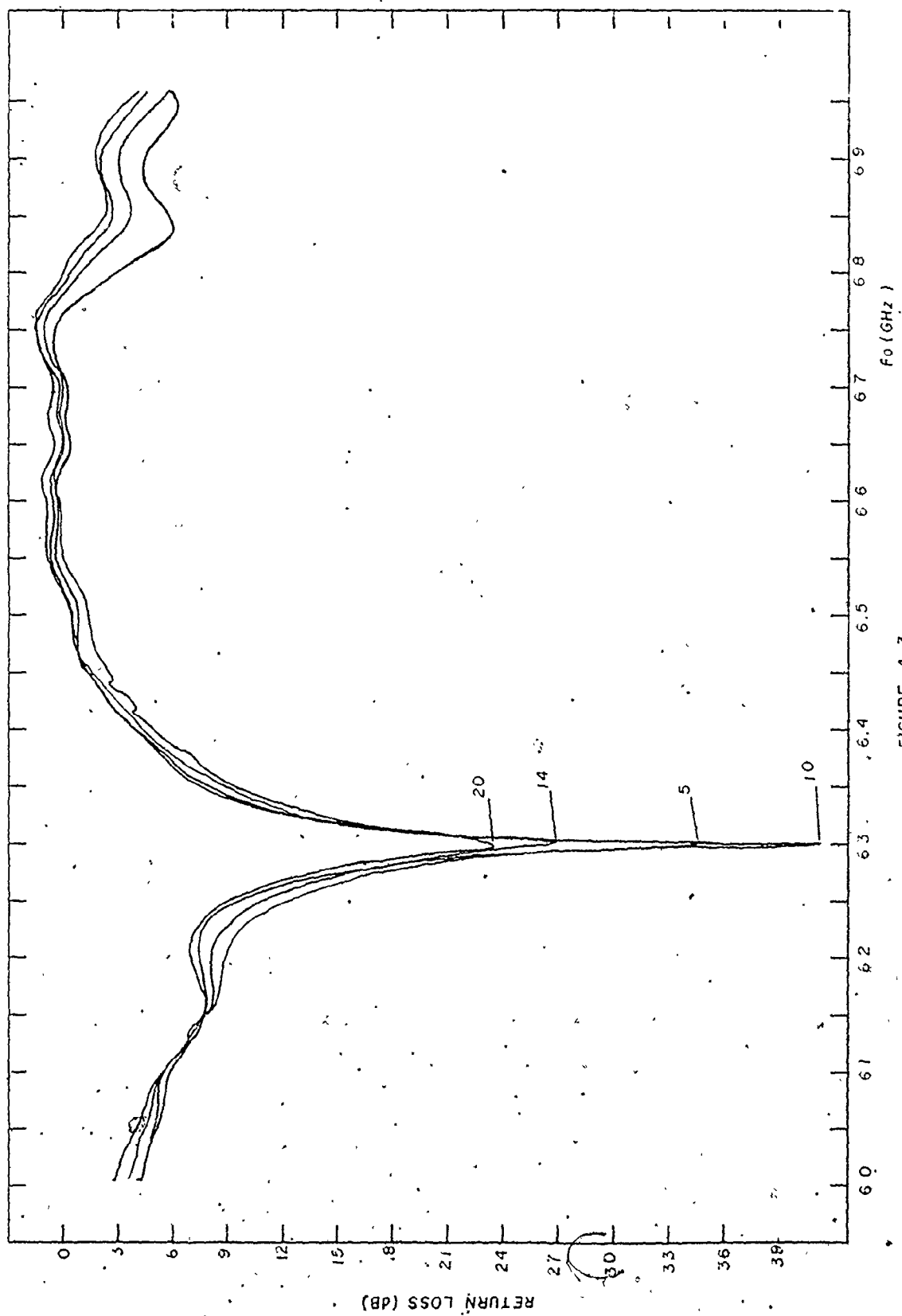


FIGURE 4.3

S₁₁ RESPONSE OF A HALF WAVE DIPOLE FOR VARYING n/w .

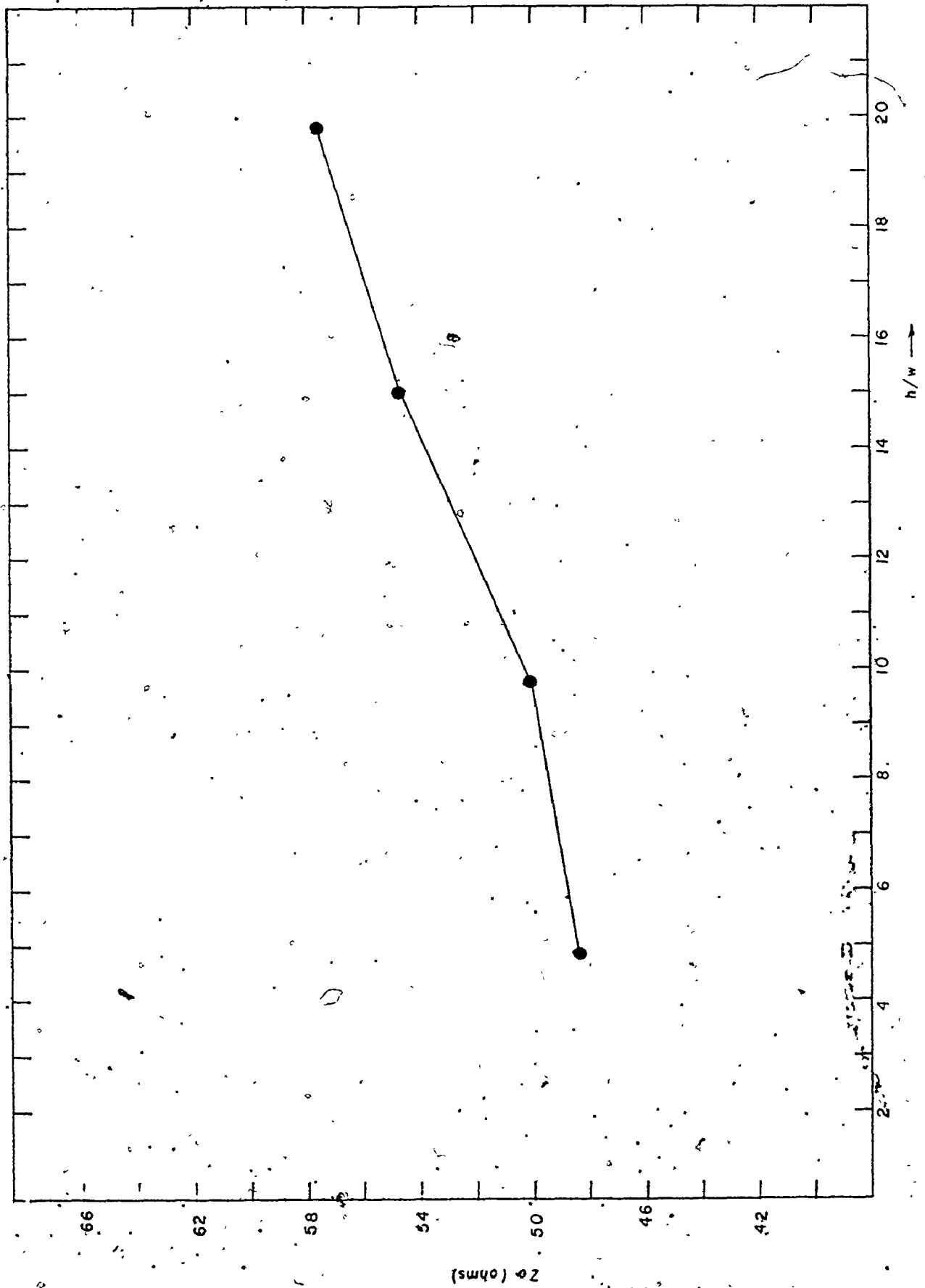


FIGURE 4.4

DIPOLE CHARACTERISTIC IMPEDANCE vs. h/w .

TABLE 4.2.1

h/w	Return Loss (dB)	$ \rho $	$ Z_a $ (ohms)
5	35	.018	48.25
10	40	.010	49.01
15	27	.045	54.68
20	23	.071	57.62

These results show that although the dipole impedance shows an increasing trend, the variation is not too far from an average of 53 ohms. The reason that these particular limits for dipole thickness were chosen was that they were within the most practical range of thicknesses that could be fabricated. Values below $h/w=5$ prove to crowd elements too closely together in the implementation of the LPDA and interelement coupling may become excessive rendering the simplified analysis of the log-periodic invalid. For $h/w>20$ the elements become too thin to be accurately etched from copper clad board as undercutting of the copper by the etchant, being relatively uncontrollable, varies h/w rapidly as elements get thinner.

This range of element widths is therefore useful for purposes of easy fabrication and, as the element impedance is not rapidly varying with h/w , good matching in LPDA design can be accomplished without worrying about variable element widths.

The second observation made from figure 4.3 is the effect of dielectric loading on the dipole. The measured resonant frequency of the element was measured as $f_{rd} = 6.3$ GHz.

The actual length of the dipole was 2.1 cm which would correspond to a free space resonance of

$$\begin{aligned} f_{ro} &= \frac{3 \times 10^{10}}{2.1 \times 2} \\ &= 7.138 \text{ GHz} \end{aligned}$$

using equation 2.3.4 the effective relative dielectric constant can be calculated as

$$\begin{aligned} \sqrt{\epsilon_{eff}} &= \frac{f_{ro}}{f_{rd}} \\ &= 1.133 \end{aligned}$$

$$\epsilon_{eff} = 1.284$$

Now knowing the values for characteristic impedance and effective dielectric constant, one may proceed in designing a log-periodic dipole array.

4.3 Design of a C-Band LPDA:

As an illustration of a typical design, an example is given here on designing a microwave LPDA for operation in C-Band.

From previous measurements, it is known that for a dipole having aspect ratio $h/w=10$, its impedance is in the region of 50 ohms and that the effective dielectric constant when using a single

sheet of dielectric board is $\epsilon_{\text{eff}} = 1.284$. Now consider the following design:

Bandwidth = 6.0 - 8.0 GHz.

Input impedance = 50 ohms

Scaling factor = .02

Spacing factor = optimum = .1714

Dipole characteristic impedance = 50 ohms

$\sqrt{\epsilon_{\text{eff}}} = 1.133$

(i) Bandwidth B = 1.333

(ii) Structure half-angle = 6.657°

(iii) Bandwidth of active region = 1.521

(iv) Structure bandwidth = 2.028

(v) Number of elements N = 10

A table listing the dimensions of all elements is given in table 4.3.1

TABLE 4.3.1

Dipole Number	L_n (mm.)	d_n (mm.)	W_n (mm.)
1	11.03		1.103
2	10.15	3.73	1.015
3	9.33	3.48	0.933
4	8.59	3.20	0.859
5	7.90	2.94	0.790
6	7.27	2.71	0.727
7	6.69	2.49	0.669
8	6.15	2.29	0.615
9	5.66	2.11	0.566
10	5.21	1.94	0.521

(vi) $R_o = 50$ ohms; $Z_a = 50$ ohms

$Z_o = 103.4$ ohms

Using the charts in appendix C

for $R_o = 50$ ohms. $a/b = 3.75$

Conductor width = 2.98 mm.

for $Z_o = 103.4$ ohms $a/b = 1.40$

Conductor width = 1.11 mm.

To feed that array, it was decided that a mode converter be used as, in this example, concern is made only over the input impedance of the array as a function of frequency. The length of the mode converter was made equal to 10 cm. as this is twice the wavelength of the lowest operating frequency: 6.0 GHz.

From section 4.2, the conductor widths on the mode converter are the same:

ground plane width = 6.9 mm.

top microstrip conductor width = 2.3 mm.

balanced line width = 2.98 mm.

The finished structure is shown in figure 4.5.

The input impedance, as measured on the network analyser, is illustrated on the Smith charts shown in figure 4.6. As can be seen from the plots, a very good match is obtained for frequencies extending past 8.0 GHz. up to about 9.3 GHz. This extension of the range in which a good match is available is very likely to be due to the larger structure bandwidth B_s as opposed to the design bandwidth B .

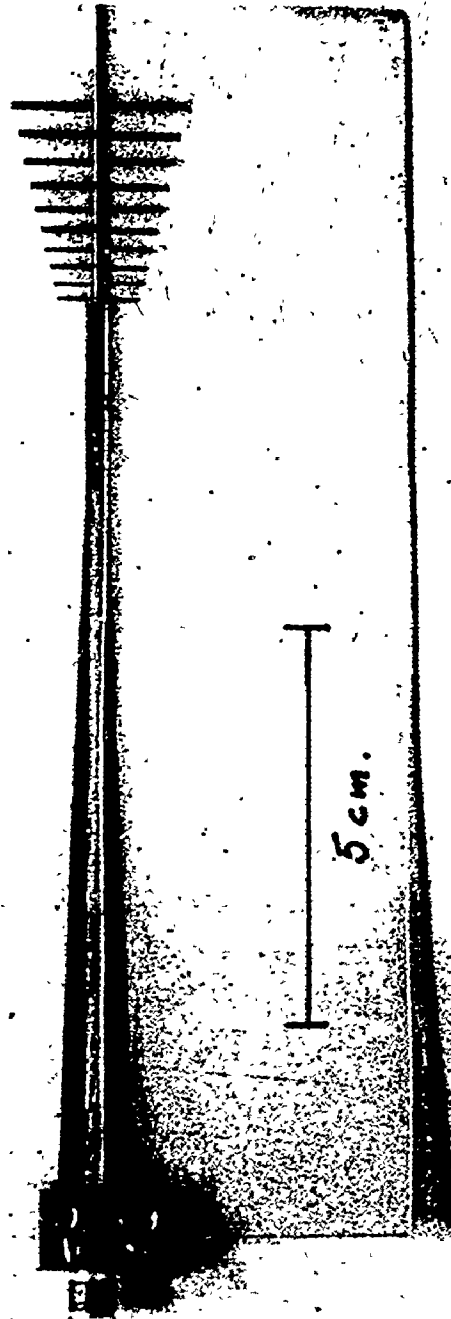


FIGURE 4.5
C-BAND LPDA FED FROM MODE CONVERTER.

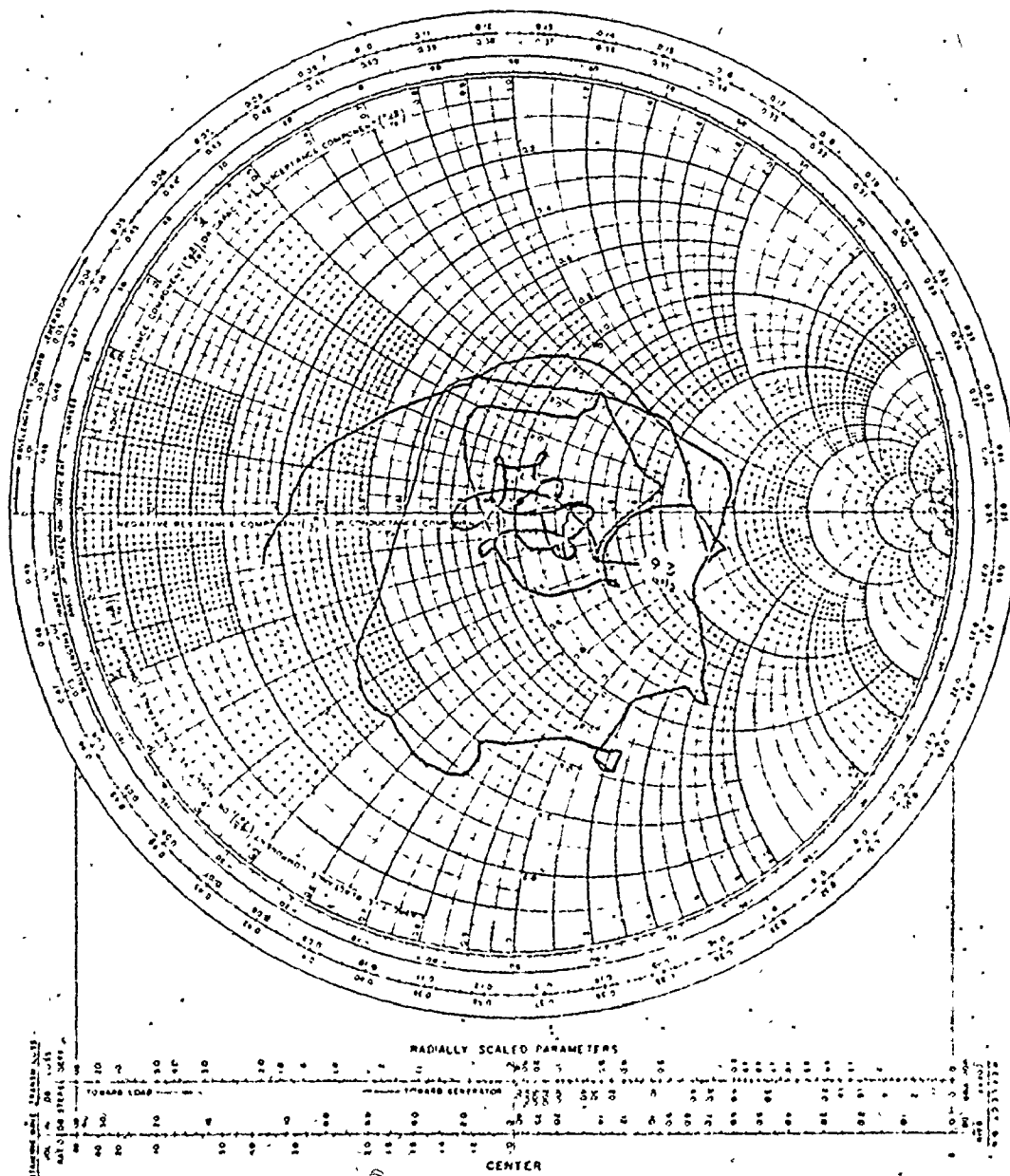


FIGURE 4.6b

S₁₁ RESPONSE 8.0 - 12.4 GHz.

4.4 Testing of the Baluns:

With the success of the prototype C-band antenna, it remained to test the operation of the reflection balun, described in section 3.2, and, if it worked properly, combine it with the log-periodic array.

The first device which was built was a fairly large sized balun constructed especially for the reason that it was desired to measure the voltage levels and phase relationships directly using the high impedance probes on a Tektronix type 454 oscilloscope. The bandwidth of the scope is 250 MHz, so a signal of 100 MHz. was applied to the balun giving the results shown in figure 4.7. The results shown looked promising at this point as the magnitudes of the voltages on each branch of the balanced line were the same with respect to ground and the phase of one branch voltage was shifted 180° from the other branch voltage. This would imply that the voltages and, hence, the currents in each branch were balanced with respect to ground.

Further measurements on the time domain reflectometer revealed, however, that although the currents may have been balanced, there was a characteristic transformation of impedance level where the incident signal on the shielded microstrip is transferred to the balanced line. This transformation of impedance is shown in the T.D.R. trace illustrated in figure 4.8 (a) which was obtained from a reflection balun having centre conductor impedance equal to 50 ohms and balanced line impedance equal to 50 ohms. There was an apparent mismatch of 50 to 12.5 ohms as indicated by the reflection coefficient of $\rho = -.6$. To test this phenomenon further, it was reasoned that if there was

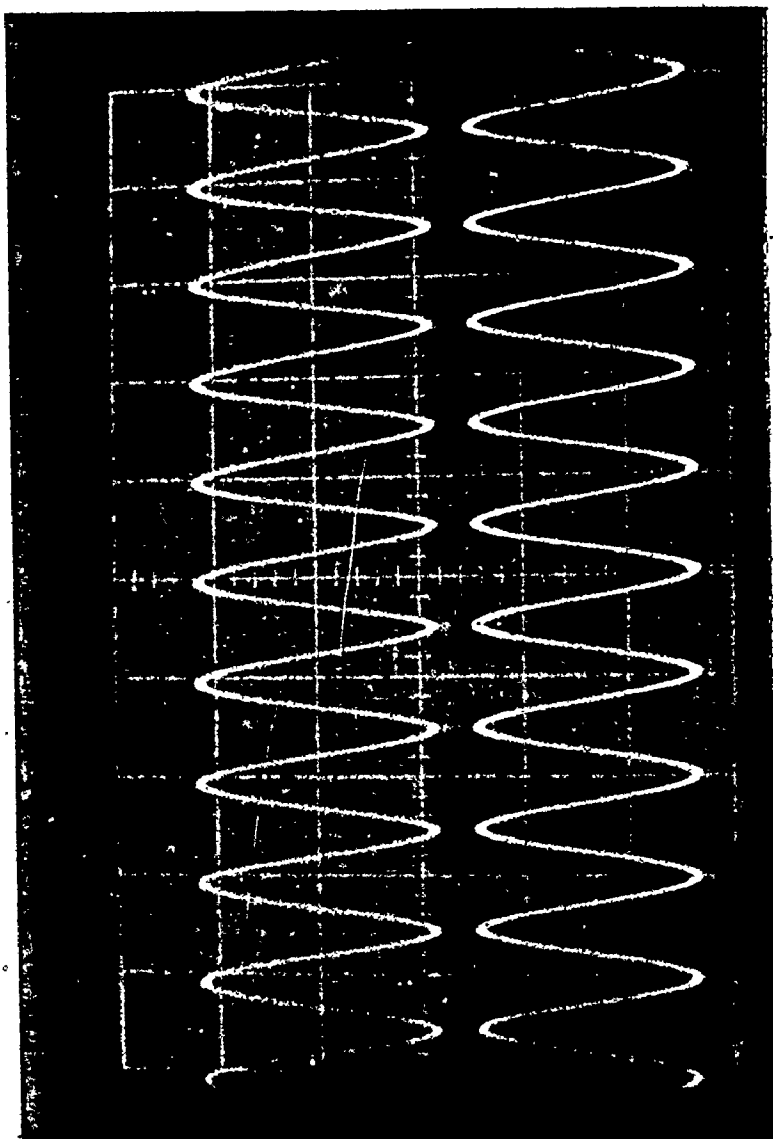
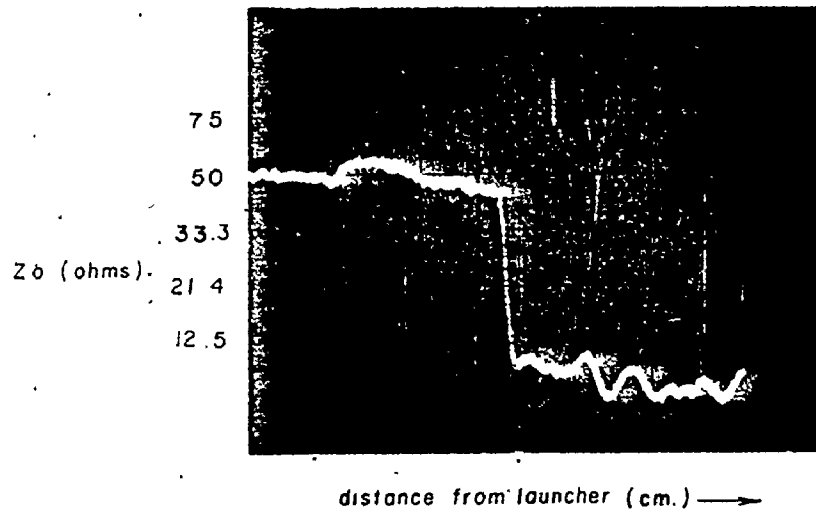


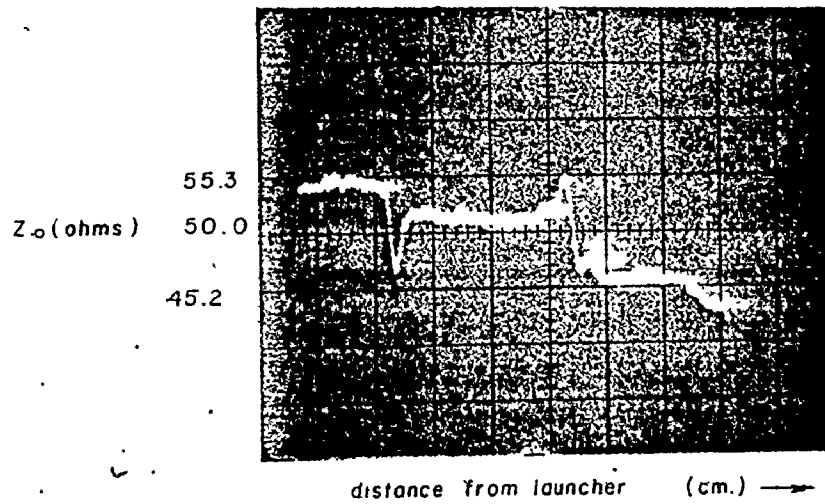
FIGURE 4.7

VOLTAGES WITH RESPECT TO GROUND ON BALANCED LINE
OF 100 MHz. REFLECTION BALUN.



(a)

50 ohm - 50 ohm Balun



(b)

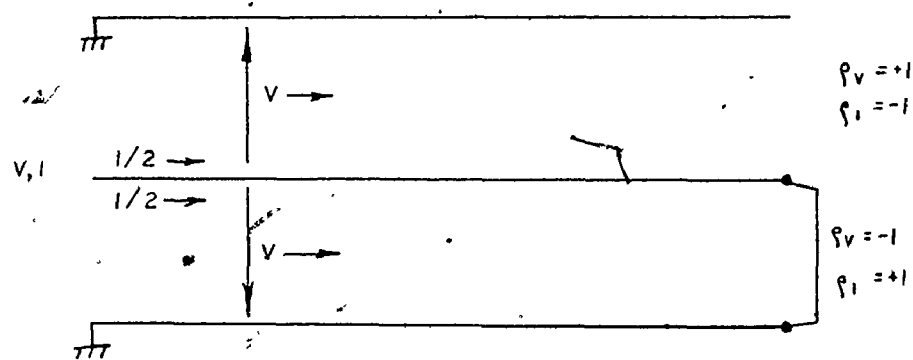
50 ohm - 200 ohm Balun

FIGURE 4.8

REFLECTION FROM 50 & 200 OHM BALANCED LINES.

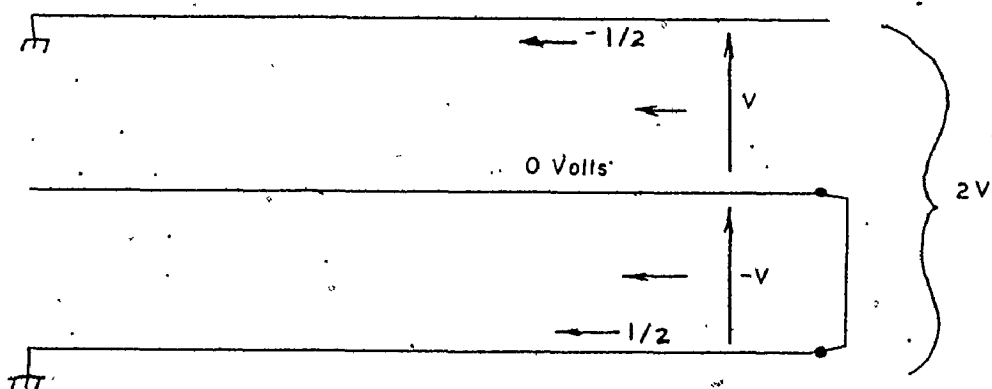
a four to one change in impedance, then a balanced line of 200 ohms would appear as 50 ohms to the centre conductor. The result of the implementation of the 50 ohm - 200 ohm balun is shown in figure 4.8b which indeed shows a good match. It now remains to explain why this phenomenon occurs.

Consider again the situation involved with the reflection balun shown in figure 4.9. Let the incident voltage and current on the shielded microstrip be V and I . Then, for a wave propagating down the line, there is a potential drop of V volts from the centre conductor to each of the ground planes. The return path for current I is split equally between the two ground planes so that each plane is carrying a current equal to $I/2$ back to the source. Observe that in this coaxial type of arrangement, one may consider the currents $I/2$ to be flowing on the inside, that is, the side facing the centre conductor, of the ground planes since there is no electric field generated on the exterior of the structure and no current flows outside. Upon reaching the end of the structure, the two voltages on the upper and lower halves of the centre conductor encounter reflection coefficients of $\rho = +1$ and $\rho = -1$ at the open and short circuit terminations respectively. The resulting situation, illustrated in figure 4.9b, shows that, after reflection, there is a voltage drop of $2V$ volts between what are now the balanced conductors with each conductor still carrying only $I/2$ amperes. Remember now that the relationship between the incident current and voltage is such that $V/I = 50$ ohms. Now, after reflection, the relationship has changed so



(a)

Incident Case



(b)

Reflected Case

FIGURE 4.9

VOLTAGE & CURRENT DISTRIBUTIONS OF INCIDENT & REFLECTED
WAVES ON THE REFLECTION BALUN.

that:

$$\begin{aligned} Z &= \frac{2V}{I/2} \\ &= 4 \times \frac{V}{I} \\ &= 200 \text{ ohms} \end{aligned}$$

In other words, the voltage-current combination is such that the propagating medium must be 200 ohms to provide reflection-free transfer of energy from the shielded microstrip to the balanced conductors. The overall effect is then the attempt to force a voltage-current characteristic of 200 ohms onto a 50 ohm line giving the observed reflection coefficient of $\rho = -.6$.

The solution to this problem is merely one of increasing the impedance of the balanced conductors four-fold to accommodate the new voltage-current relationship. Even though the impedance step-up can be compensated for, the higher impedance and, therefore, the narrower conductor widths cause some practical problems.

First of all, if one considers trying to match an LPDA with 50 ohm dipoles to the 200 ohm balanced line, it is found from equation 2.4.12 that the impedance of the array feeder must be of the order $Z_0 = 400$ ohms. Such a high impedance level forces the array feeder width to become quite narrow which causes some problems during implementation. Firstly, when considering the propagation of the incident wave down the shielded microstrip, the fact that the ground planes in the region of the array feeder become narrow would cause a deviation

in the characteristic impedance of the microstrip. The change in impedance comes about from the ground plane width being of the same order as the centre strip, allowing substantial fringing to occur around the ground planes forcing a new mode of propagation, with its own characteristic impedance, to be set up. This is one source of mismatch due to the addition of an antenna array onto the balun. Another disturbance is caused by the elements in the array which periodically load the balanced line. If the case becomes such that fringing occurs around the ground planes as just described, it is very likely that some of the incident energy propagating down the centre strip may be coupled out by resonant elements, or reflected by reactive elements in the array, thus causing a degradation in signal integrity even before it reaches the feedpoint of the antenna.

It was for these reasons that the reflection balun was abandoned as a viable method of feeding the log-periodic array. A second involving the mode converter as the source of a balanced signal was devised, however, and proved to be successful in feeding the array. The structure is shown in figure 4.10.

In this method of feeding, the entire mode converter is constructed and terminated in a balanced transmission line equal to the length of the log-periodic antenna. The balanced line is then sandwiched between two other dielectric boards which support the LPDA half structures and the balanced line of the mode converter is connected to the balanced line (of the same impedance as the mode converter) of the antenna array. By doing this, one may obtain a

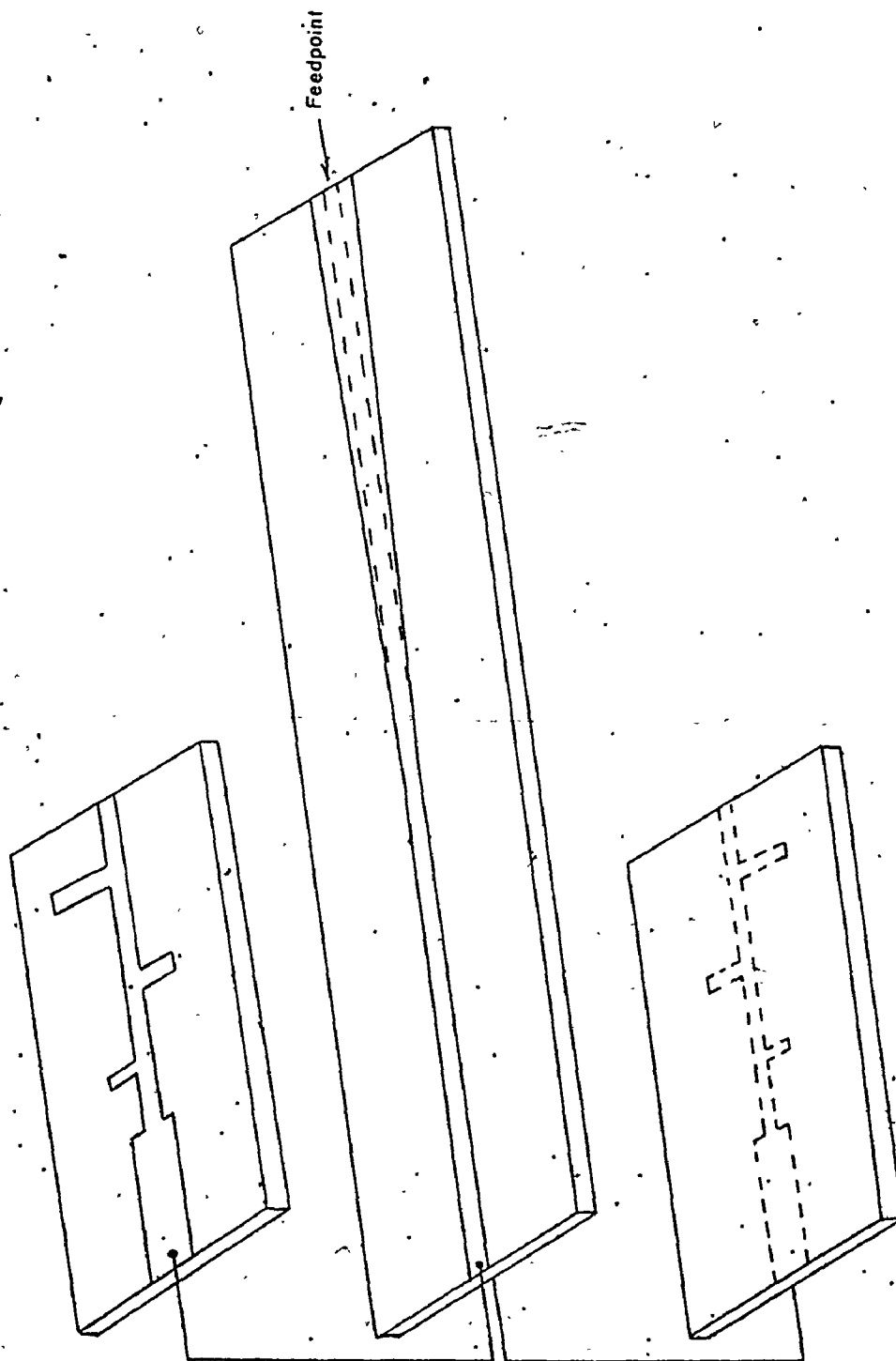


FIGURE 4.10

MODE CONVERTER FEED FOR LPDA.

balanced feed for the antenna as well as keeping the region in the direction of the main lobe free from obstructions.

It was realized that by sandwiching the balanced line of the mode converter between the balanced line of the antenna, the impedance of the mode converter line may change somewhat from its 50 ohm level. Observation of traces from the T.D.R. (see figure 4.11) showed indeed that this was the case, reducing the 50 ohm line to about 41 ohms. This was easily resolved by trimming the balanced line on the mode converter slightly so as to raise its impedance back to a constant 50 ohms.

4.5 Design of S - Band LPDA With Mode Converter Feed:

To test the mode converter type of feed, an S - band log-periodic antenna was designed for operation in the 2 to 4 GHz. band. The parameters for the structure are listed below and the element dimensions given in table 4.5.1.

Bandwidth = 2.0 - 4.0 GHz.

Scaling constant = .92

Spacing constant - optimum = 0.17136

$h/w = 10$

$\sqrt{\epsilon_{eff}} = 1.25$

Note that the correction for dielectric loading is increased in this case from the measured value of 1.133 to 1.25.

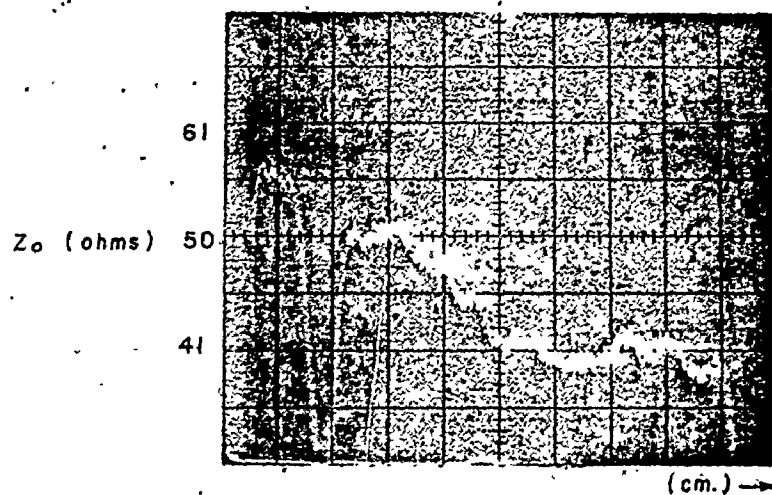


FIGURE 4.11

REDUCTION OF BALANCED LINE IMPEDANCE WHEN
SANDWICHED BETWEEN CONDUCTING PLANES.

The reasoning behind this was that it must be true that the additional dielectric supporting the stripline between the half planes of the antenna array loads the dipoles to some extra degree. Thus the loading factor was increased by a trial amount and the effect observed upon testing the structure.

Again, following the method in section 2.5:

- (i) $B = 2.0$
- (ii) Structure half angle = 6.66°
- (iii) $B_{ar} = 1.521$
- (iv) $B_s = 3.042$
- (v) Number of elements $N = 15$
- (vi) $R_o = Z_a = 50$ ohms $Z_o = 102.5$ ohms
 balanced conductor width = 8.93 mm.
 antenna feeder width = 3.33 mm.

TABLE 4.5.1

Dipole Number	L_n (mm.)	D_n (mm)	W_n (mm.)
1	29.97		2.997
2	27.58	10.27	2.758
3	25.37	9.45	2.537
4	23.35	8.69	2.335
5	21.48	8.00	2.148
6	19.76	7.36	1.976
7	18.18	6.77	1.818
8	16.72	6.23	1.672
9	15.38	5.73	1.538
10	14.16	5.27	1.416
11	13.02	4.85	1.302
12	11.98	4.46	1.198
13	11.02	4.11	1.102
14	10.14	3.78	1.014
15	9.33	3.47	0.933

The measurement of the input impedance of the device, shown on the Smith chart in figure 4.12, illustrated that a good match did not occur for frequencies below approximately 3.0 GHz. This was most likely due to too high a value for the dielectric loading factor. Above the 3 GHz. mark it can be seen that a good match to the coaxial line was made with standing wave ratios within 1.5:1 and a mean resistance level as defined by Carrel (3) of $R_0 = 52$ ohms.

By observing how much higher in frequency the structure began to match, the value of the dielectric loading factor was recalculated as being $\sqrt{\epsilon_{eff}} = 1.176$. With this in mind, a second array having the same bandwidth and impedance levels was constructed taking into account the new dielectric loading factor.

The input impedance of the new device, shown in figure 4.13, is again close to being a resistive value of $R_0 = 50$ ohms as desired. This particular array showed a VSWR not greater than 1.8:1 in the range 2.05 to 4.2 GHz. and a mean resistance value of 60 ohms. The pass band also now extends down to almost 2 GHz. as was originally planned.

Swept frequency measurements of the antenna radiation pattern in both the E and H planes were made and are shown in figures 4.14 through 4.17. The first observation one might make here is the anomalous behaviour of the array around 2.3 GHz. in which a fairly deep notch occurs between $\pm 60^\circ$ and $\pm 80^\circ$ and a fairly predominant increase in the backlobe level for angles $\pm 90^\circ$ to $\pm 180^\circ$ in both the E and H planes. It must be made clear, though, that during the manufacture of the array, the third longest monopole element in one

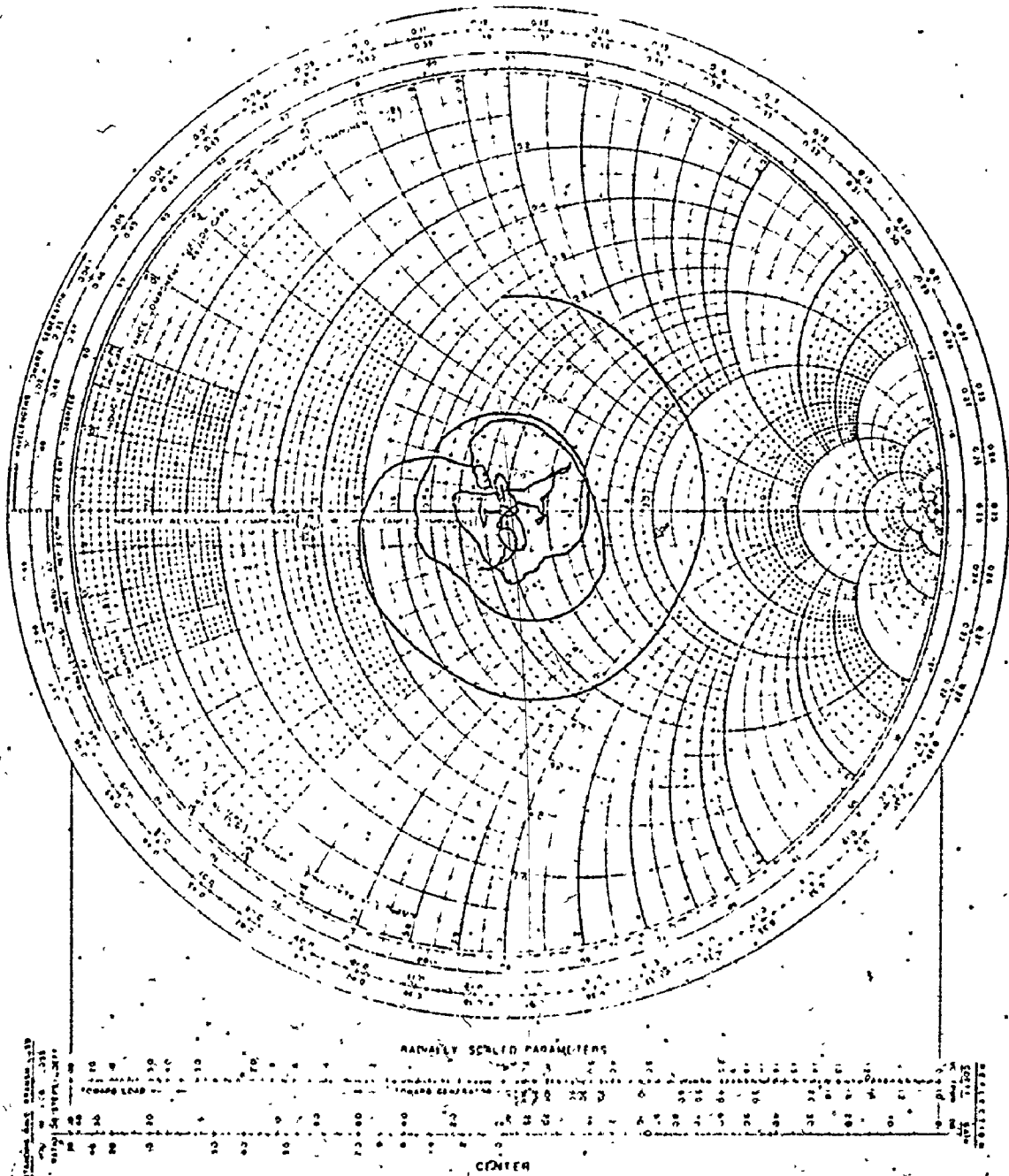


FIGURE 4.12

SW RESPONSE 18 - 4.2 GHz

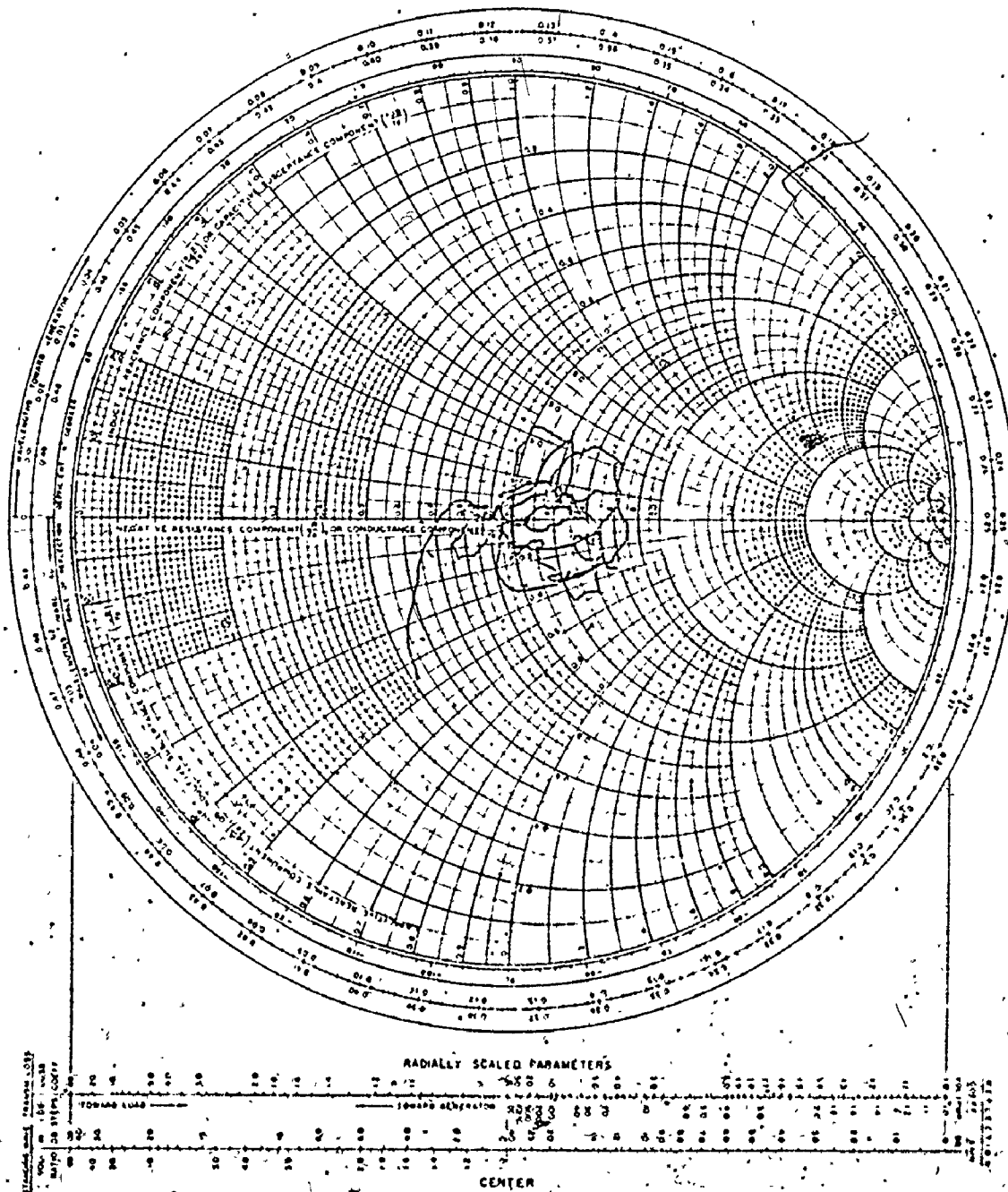
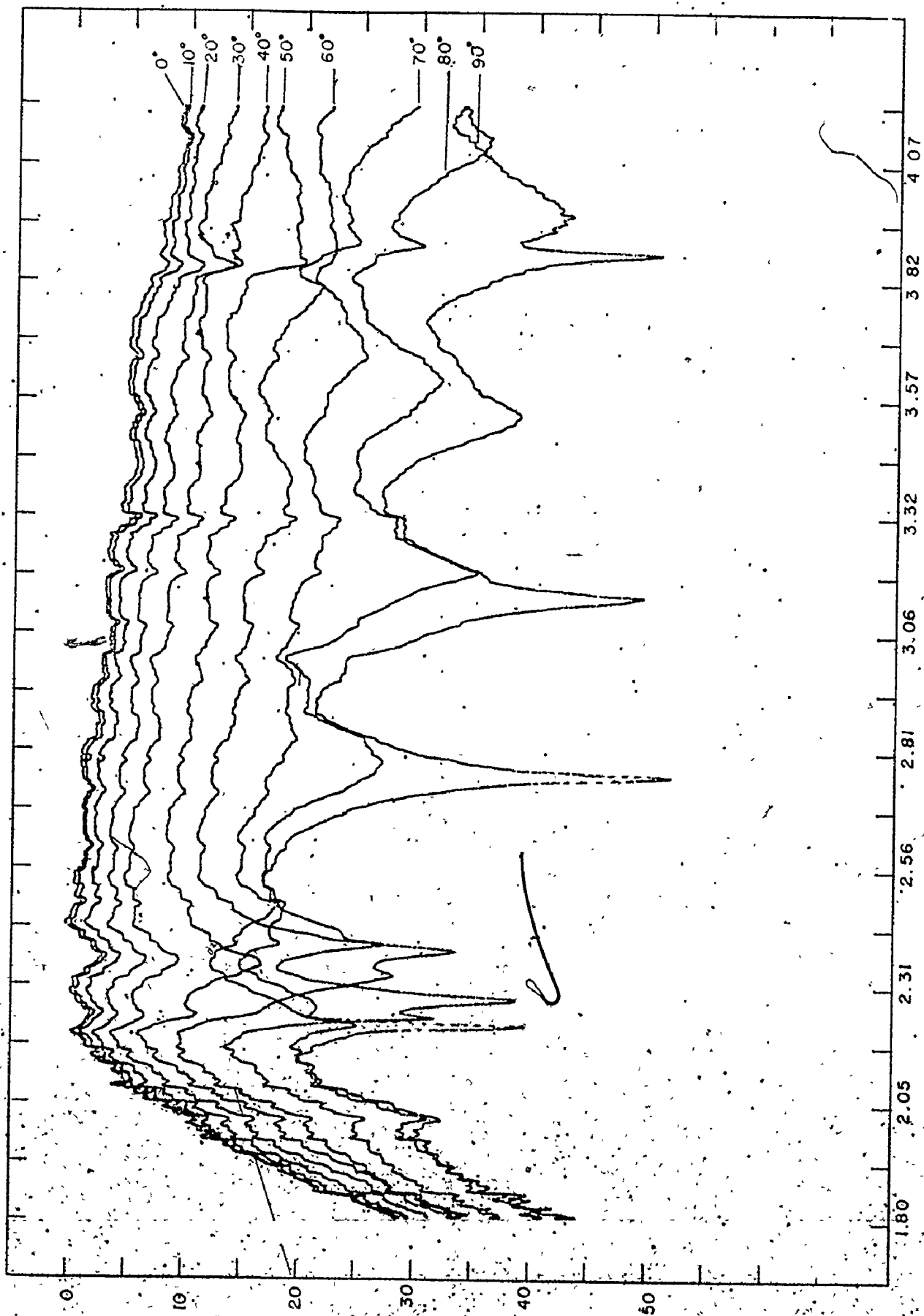


FIGURE 4.13

S₁₁ RESPONSE 1.6 - 4.2 GHz



F (GHz.)

FIGURE 4 14

H-PLANE RADIATION PATTERN FOR S-BAND LPDA (0° 90°)

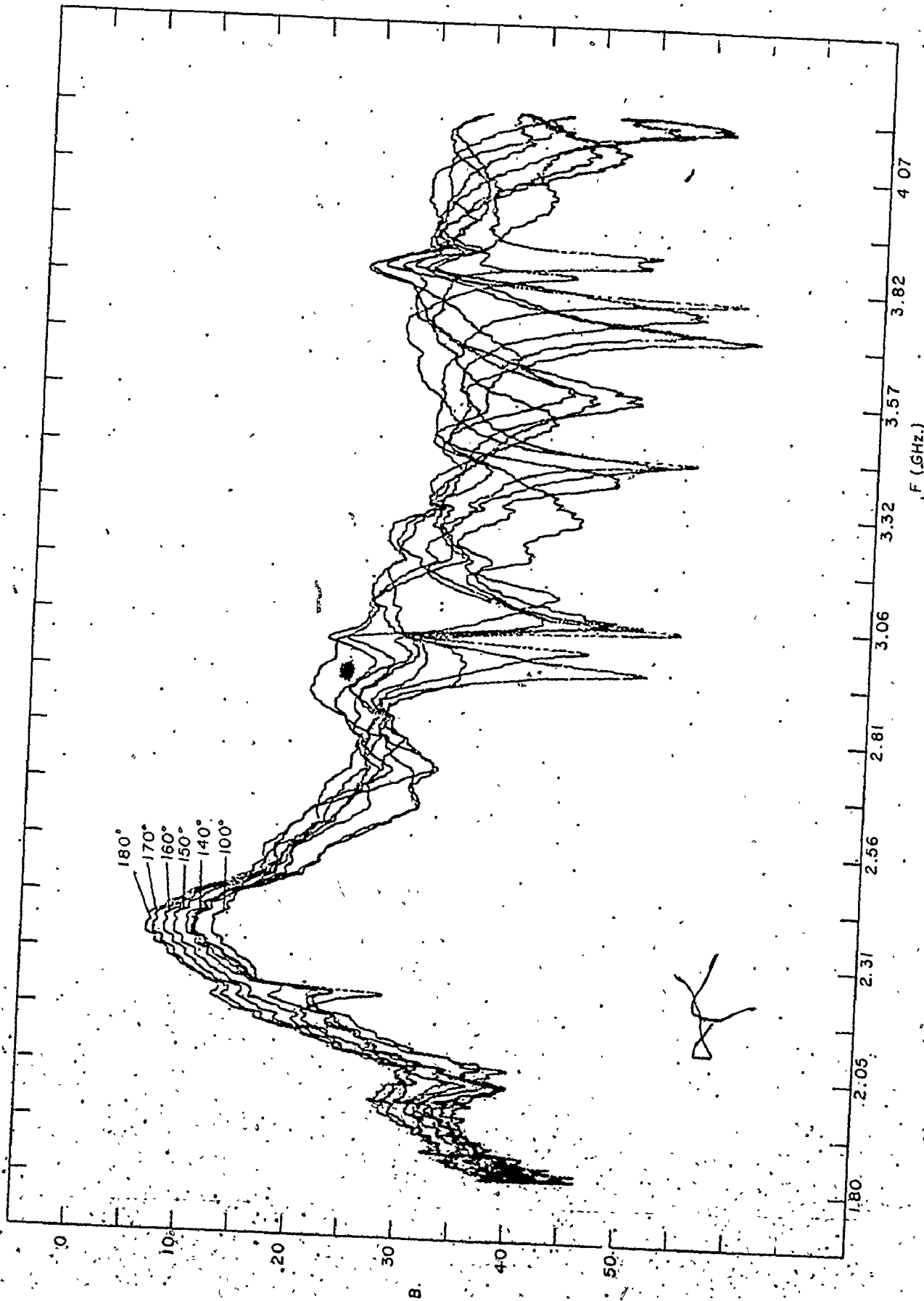


FIGURE 4.15
H-PLANE RADIATION PATTERN FOR S-BAND LPDA (100° - 180°)

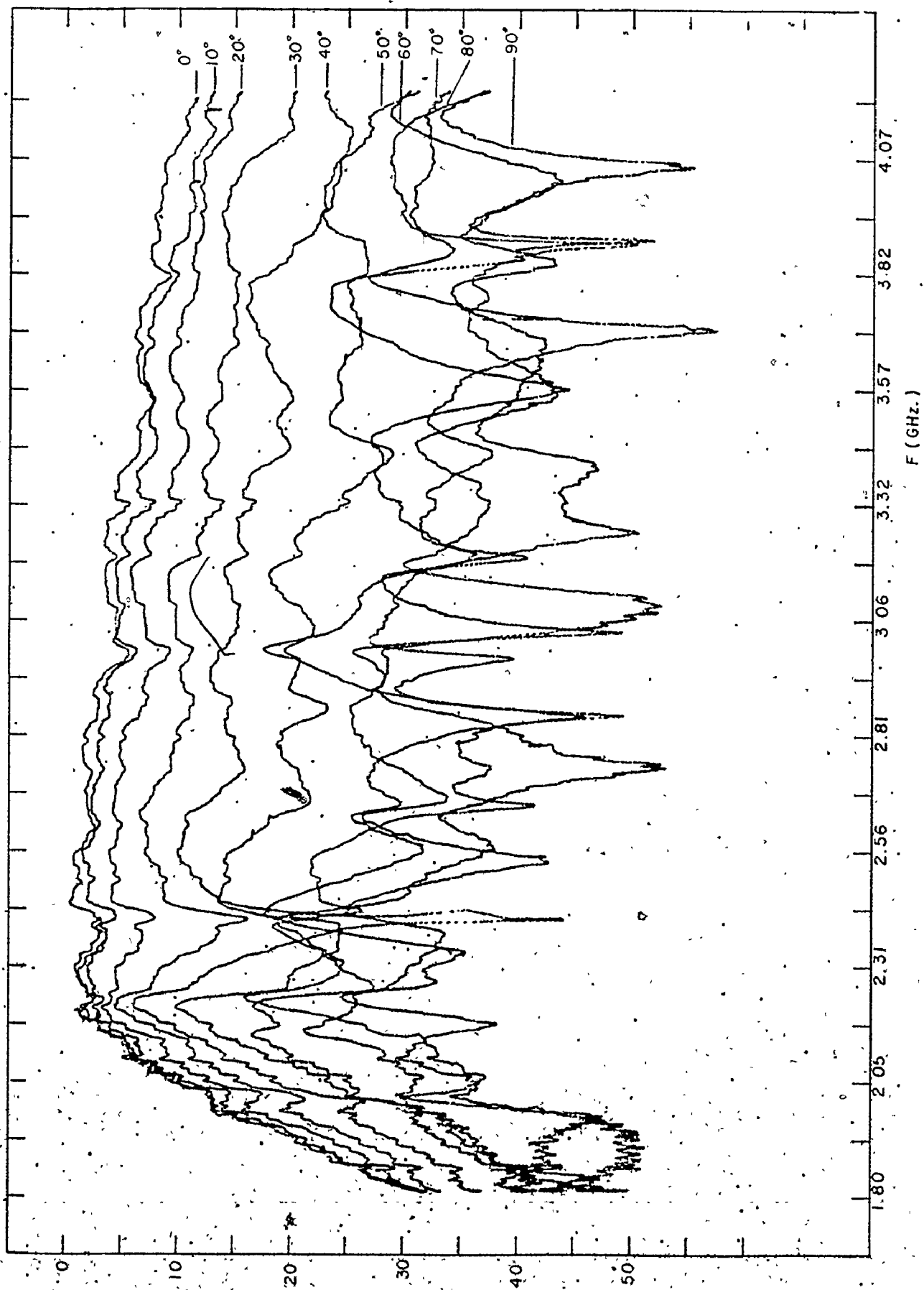


FIGURE 4.16
E-PLANE RADIATION PATTERN FOR S-BAND LPDA ($0^\circ - 90^\circ$)

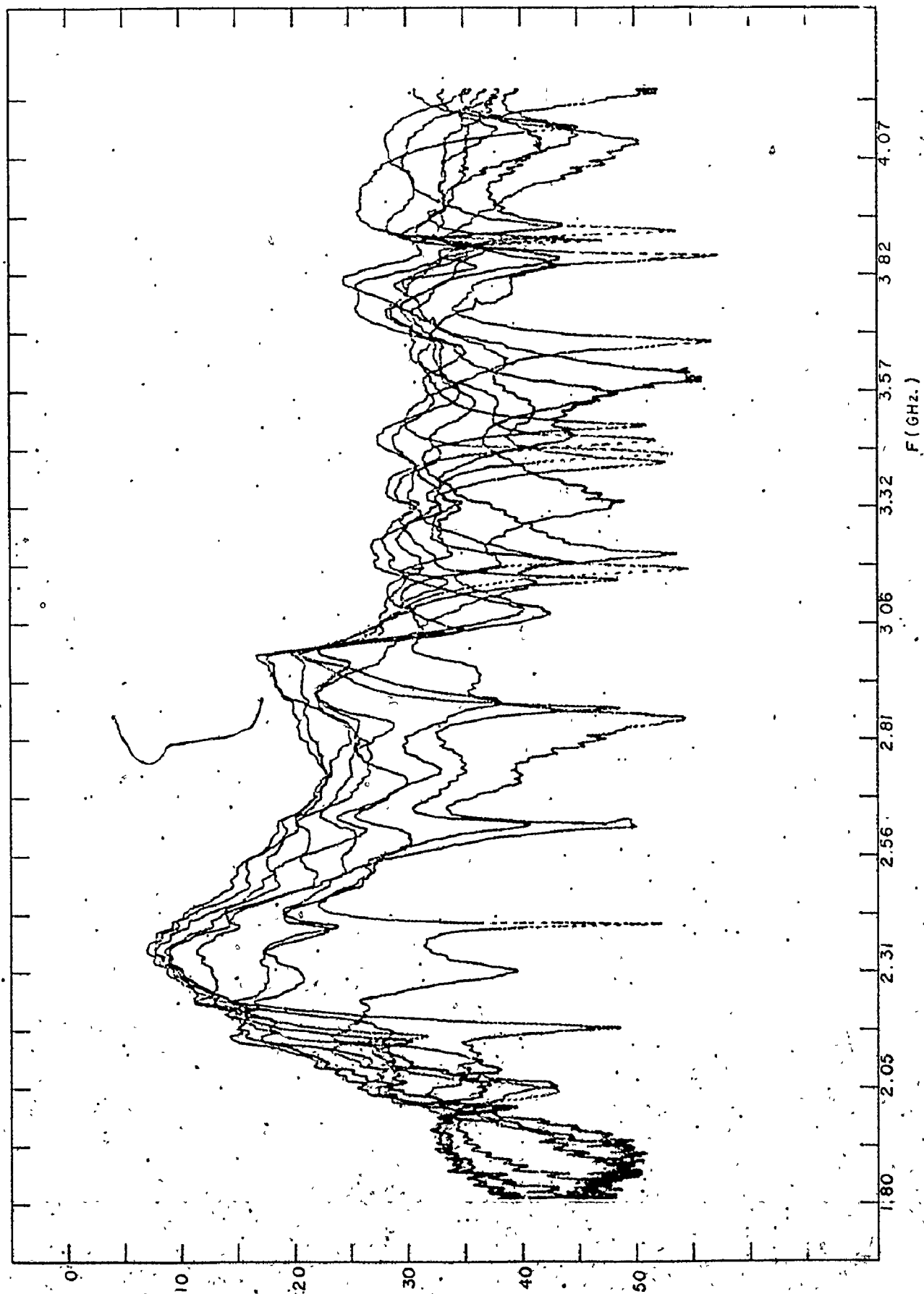


FIGURE 4.17

E-PLANE RADIATION PATTERN FOR S-BAND LPDA ($100^\circ - 180^\circ$)

half of the array was shorter than its counterpart in the other half plane. This asymmetry in the dipole was researched by Balmain and Nkeng (22) and the results shown here are very similar to those caused by an unsymmetric dipole in a log-periodic antenna array. The required length of the element in question was 26.95 mm. which, when taking into account the dielectric loading, corresponds to a frequency of 2.36 GHz. It would appear, then, that this element was the cause of the anomalous behaviour of the antenna at the low end of its operating band.

Otherwise, the array showed a very well defined front lobe in both the E and H planes extending in the backfire direction as desired. The measured front - to - back ratio was fairly constant at about 20 dB. and was never less than 15 dB. The directive gain of the antenna was calculated from the approximate formula:

$$D = 10 \log \frac{41,250}{W_e \times W_h}$$

where W_e and W_h are the 3 dB. beamwidths of the major lobe in the E and H planes respectively, and D is the directivity expressed in decibels (4). In this case the directivity is found to be of the order of 23 dB. The value is rather high, being more than double the value quoted by Carrel for a free space structure having the same spacing and scaling constants.

A possible reason for the high directivity could be that the containment of the electric field by the dielectric in the

neighbourhood of the antenna caused a squeezing of the main lobe into a narrower beam than might have been expected.

CHAPTER V

CONCLUSIONS.

From the results and discussions in Chapter 4, it may be said that the notion of being able to construct logarithmically periodic dipole antenna arrays on a dielectric substrate is a valid one.

It may be true that because of the inherently small aperture provided by a half wave dipole at microwave frequencies, an M.P.C. log-periodic dipole array may not be desirable for receiving purposes alone because of its inability to intercept a reasonable amount of energy from the source of radiation. This drawback is not very serious though since it is always possible to use the array in conjunction with a parabolic dish reflector which serves as a collector for the energy. The energy could then be focused by the dish to a log-periodic array at the feed point. The reason for using a log-periodic array instead of a conventional dipole or horn antenna lies in the fact that it is frequency independent (or nearly so) and is the only element required at the feed point for any received frequency. This would eliminate the need for multiple off-axis feed points and dichroic filters which clutter up the dish aperture. The small size and high resistance to mechanical distortion also make this device conducive to dish applications.

Some remarks should also be made here concerning the reflection balun which was examined in Chapter 4. It was found, that because

of the four to one increase in the required impedance of the balanced line feeding the antenna, the line feeding the dipoles of the array becomes too narrow to maintain a ground plane for the centre strip of the balun. It was considered later that the possibility exists of tapering the balanced line from the end of the balun to a lower impedance at the feed point of the array thereby necessitating a lower dipole feeder impedance and hence widening the dipole feeder and re-establishing the ground plane condition. This may be done by using the optimum Dolph-Chebyshev taper mentioned before and given in Appendix D. By using this taper, a smooth transition with minimum reflection coefficient could be made from the 200 ohm value at the balun end to 50 ohms (say) at the feedpoint of the antenna array.

APPENDIX A

FORTRAN IV PROGRAM FOR DESIGNING
M.P.C. LOG - PERIODIC ANTENNAS.

The listing given below was that used for designing the antennas in this thesis. It mainly follows the design procedure in sections 2.3, 2.4 and 2.5.

[illegible]

APPENDIX B

THE PHOTO - ETCHING TECHNIQUE

The first step in the photo-lithographic process is to lay out and cut the pattern of the desired antenna array from a positive masking material. This was done on a commercially available mask known as Ulano Rubylith #1492, red on clear plastic transparency. Cutting of the mask was facilitated through the use of a precision cutting table (Haag-Streit Coordinatograph).

Once proper coordinates are set up on the cutting table, the mask is cut out in such a way as to leave the red overlay where the copper is to remain on the finished board. This is because the developing technique describe later uses a positive mask during exposure.

Once the mask is cut out, making sure that no pin holes are present in the red overlay, the copper clad board is prepared for exposure. First, the board is scrubbed clean on all sides which are to be exposed with an abrasive cleanser, such as 'Comet'. Having done this, the board is then scrubbed with tripoli abrasive powder to remove any gross scratches which may be present. Following this, the board is then rinsed with acetone, trichloroethylene and distilled water, in that order, in order to remove any grease and skin oil which may have been deposited while handling. Once one is sure that the board has been sufficiently cleaned and degreased, a final dip into a concentrated ferric chloride solution for 30 seconds is done to remove any foreign matter left from the degreasing process and also to expose the bare copper surface free from any copper oxide.

The board is finally rinsed with distilled water and blown dry with compressed nitrogen making sure that no contact occurs between bare skin and the clean board. The dry board is then baked in an oven at 85°C for a period of 15 to 20 minutes. All procedures after this point must be carried out under a safelight which will not expose the photo-resist.

The treated board is now thoroughly coated with a positive working photo-resist liquid, such as Azoplate AZ-1350B, by dropping resist onto the surface with a medicine dropper and spinning the board at high speed on a platform. Once an adequately thick layer of resist has been applied, the board is baked further at 85°C for another period of 15 to 20 minutes.

When the resist has sufficiently been baked, the board is removed from the oven and the positive mask placed over the desired area to be exposed. The board is then exposed for at least 3 minutes under an ultraviolet light source or 7 minutes under a strong projection lamp after which the mask is removed and the board developed in a suitable positive resist developer. Developing takes about three minutes on the average and an indication of when the exposed resist is removed is given by a discolouration in that area. The board is then rinsed thoroughly under tap water and blown dry. If the board has been sufficiently developed, the exposed copper should have a chalky appearance with no apparent gloss.

After developing, the board is then dipped into an etching solution consisting of concentrated ferric chloride held at a temperature of $40 - 45^{\circ}\text{C}$. The board is agitated in this solution until

all excess copper has been removed leaving the desired antenna structure.

APPENDIX C

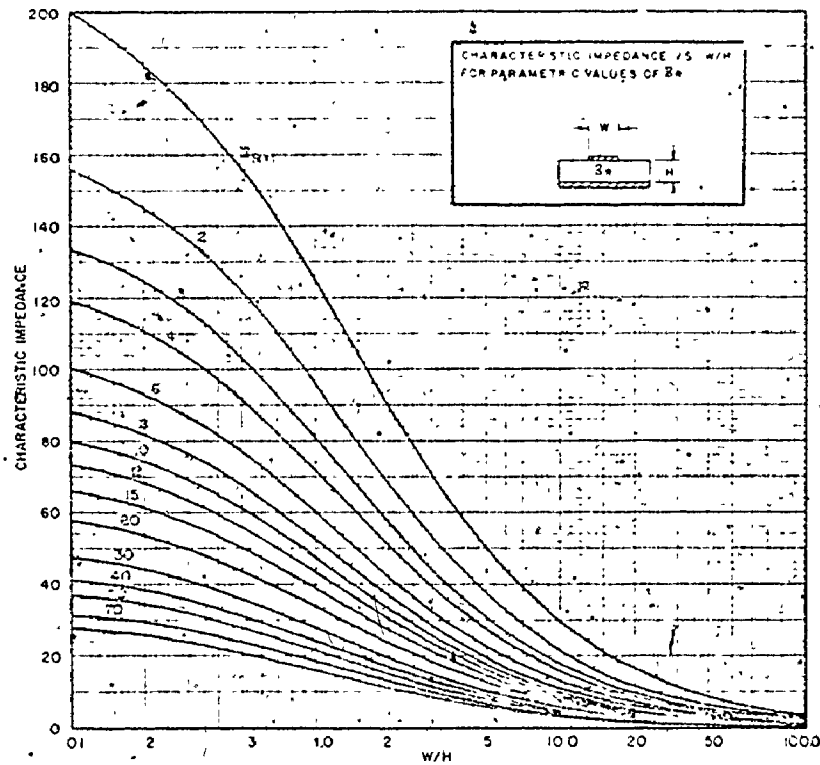
MICROSTRIP AND STRIPLINE CHARTS.

In order to get the proper impedance line in a design involving printed circuits, it is necessary to calculate the impedance values analytically for each particular geometry which may be considered.

Fortunately, for the purposes of designs involved in this thesis, characteristic impedance charts have been developed by several authors and it is only necessary to find the ones which concern themselves with the geometry of stripline desired.

The three geometries used in this thesis were (a) microstrip above an infinite ground plane, (b) balanced stripline separated by a dielectric sheet and (c) shielded microstrip. The characteristic impedance of these types of printed circuit transmission line have been analysed by Wheeler (see ref. 20) for the balanced stripline, and Hayt (see ref. 21) for the shielded microstrip line. The charts of characteristic impedance are given on the following pages.

MICROSTRIP CHARACTERISTIC IMPEDANCE CALCULATED FROM WORK OF WHEELER
WIDE STRIP APPROXIMATION ($W/H > 1$)



NARROW STRIP APPROXIMATION ($W/H < 1.0$)

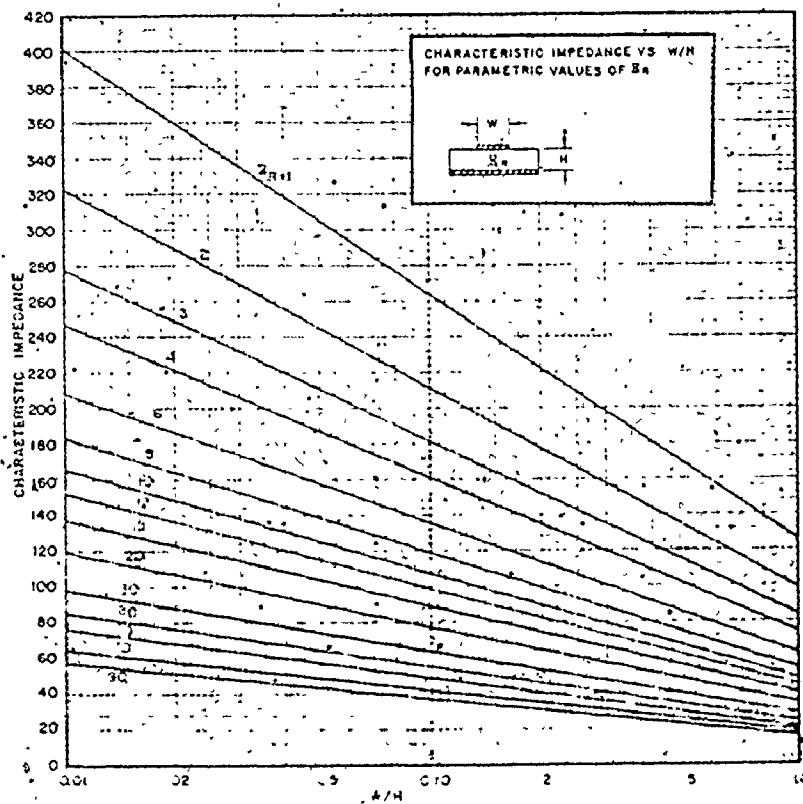


FIGURE C-1

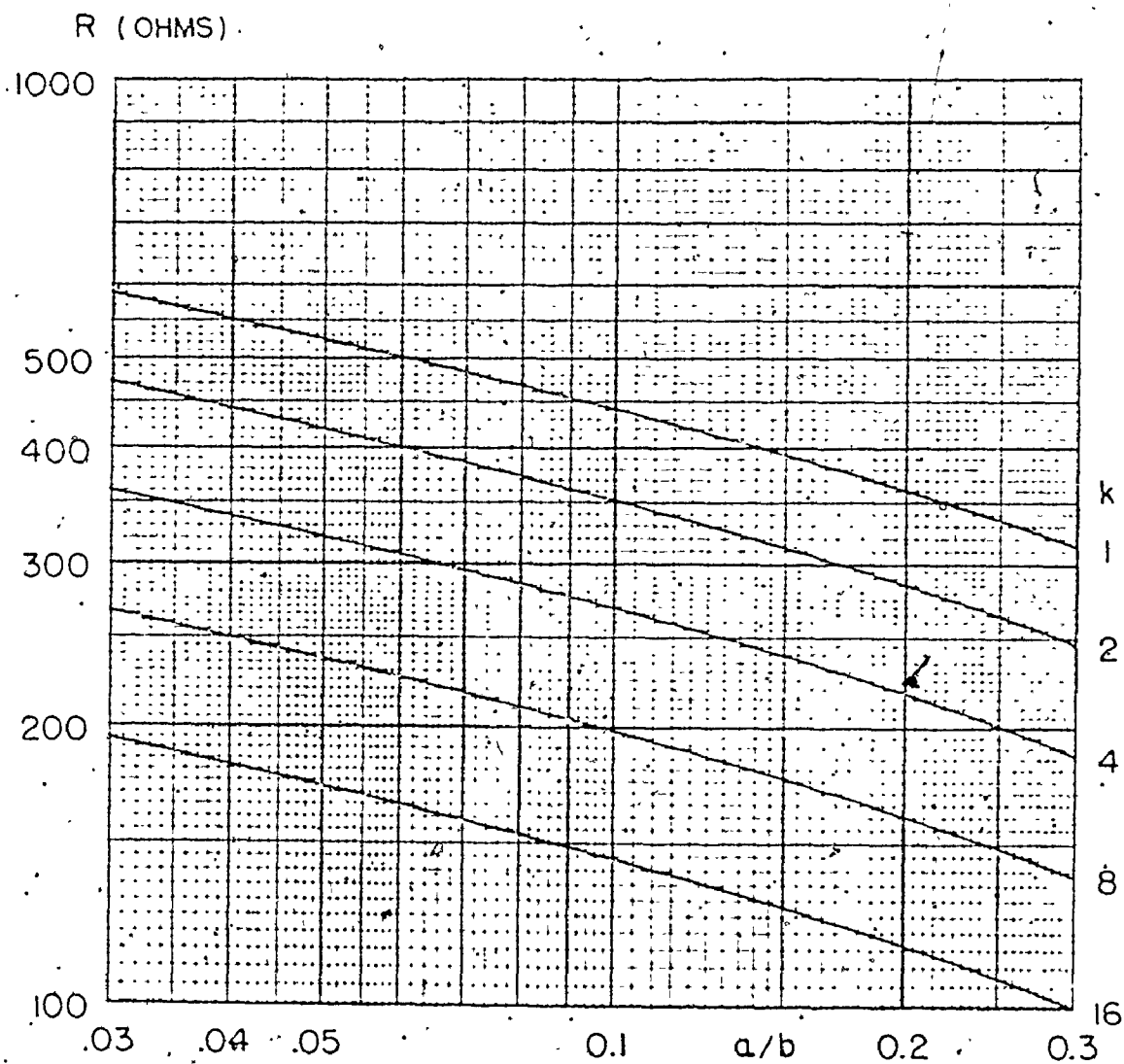


FIGURE C - 2 (after Wheeler(20))

BALANCED LINE IMPEDANCE

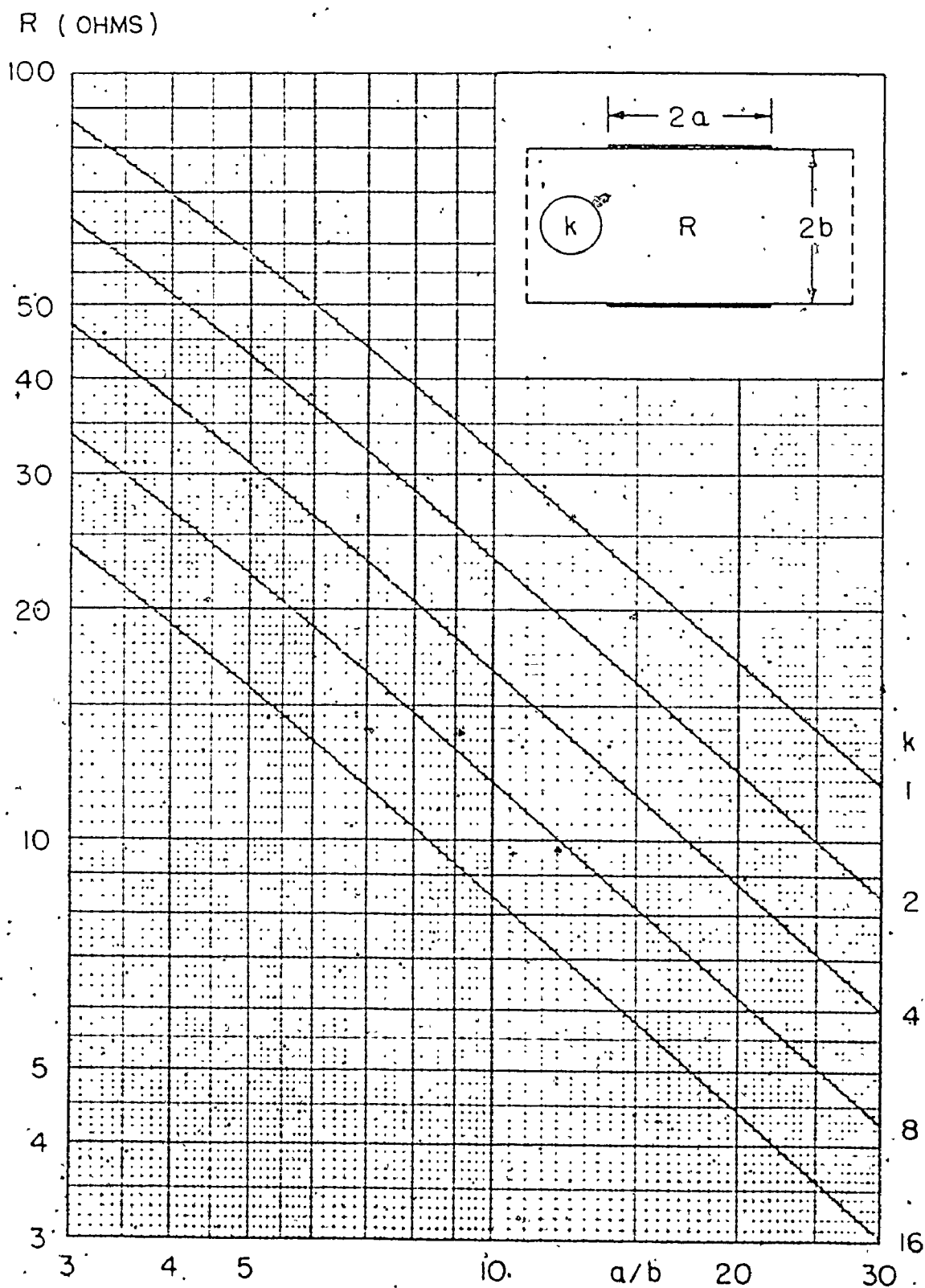


FIGURE C - 3 (after Wheeler (20))

BALANCED LINE IMPEDANCE.

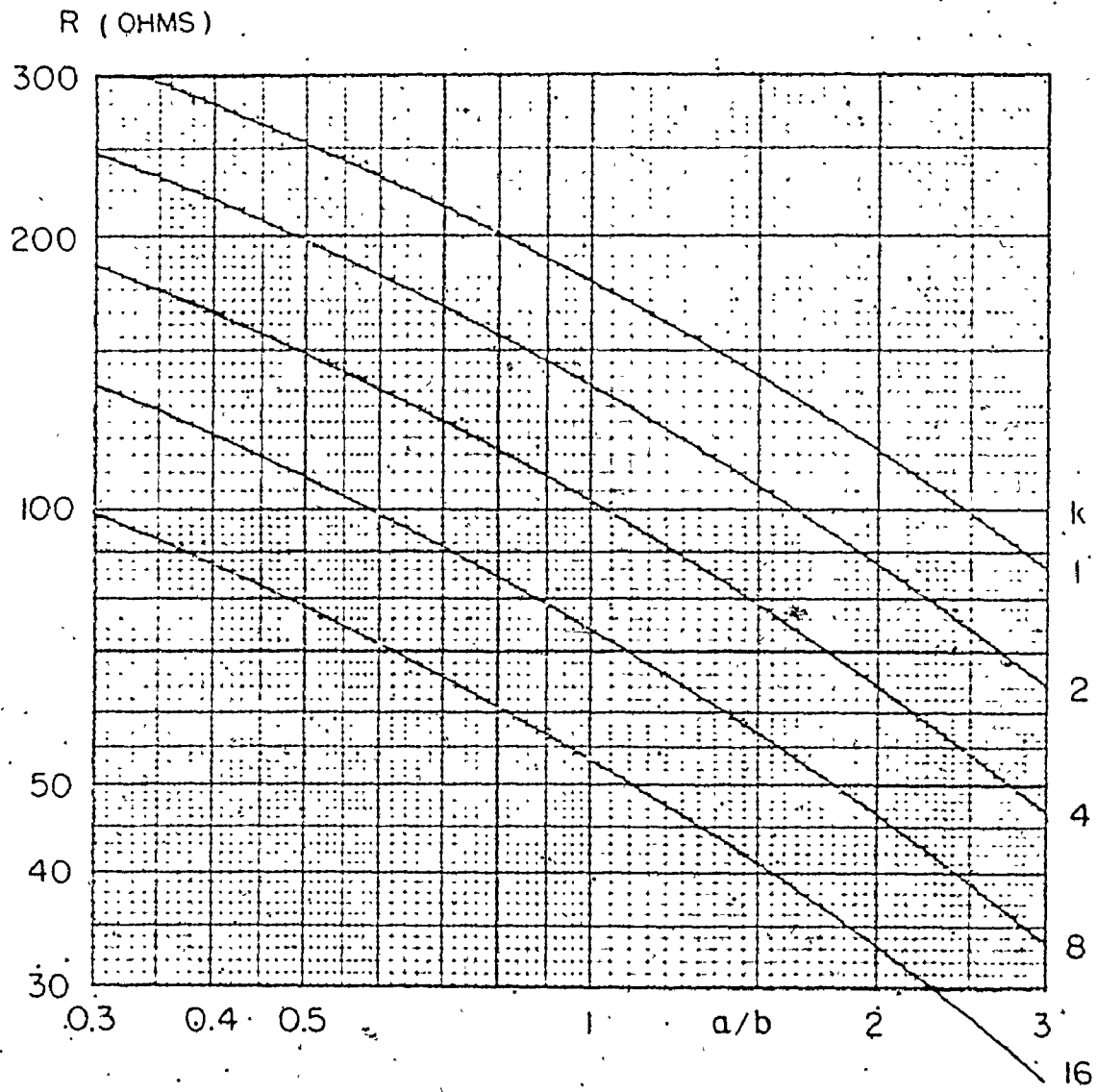


FIGURE C - 4 (after Wheeler (20))

BALANCED LINE IMPEDANCE.

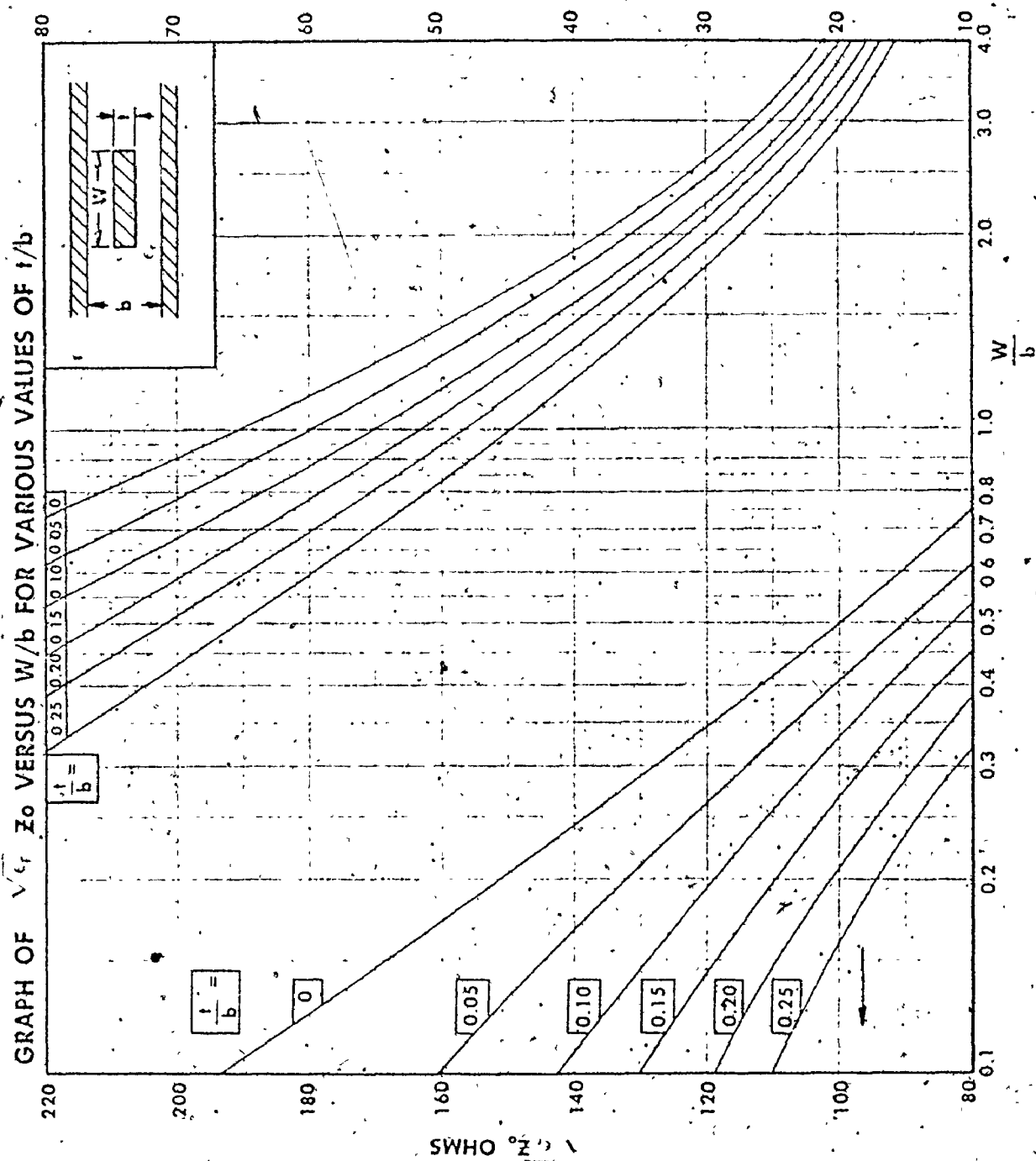


FIGURE C-5

REFERENCES.

1. KANDOLAH, A. G., "Three New Antenna Types and Applications.", Proc. of the I.R.E. Volume 34, Feb. 1946.
2. JORDAN, E. C. and K. G. BALMAIN, "Electromagnetic Waves and Radiating Systems", Second edition, Prentice-Hall Inc., Englewood Cliffs, N.J., 1968, pp. 603 - 624.
3. CARREL, R. L., "Analysis and Design of the Log Periodic Dipole Array.", University of Illinois Tech. Rept. #52, Urbana, Illinois, 1961.
4. SMITH, C. E., "Log Periodic Antenna Design Handbook.", prepared for the Bureau of Ships, U. S. Navy by Smith Electronics Inc., Cleveland, Ohio, 1961.
5. DURAMEL, R. H., and D. E. ISBELL, "Broadband Log Periodic Antenna Structures.", I.R.E. 1957 National Convention Record, Part I pp. 119 - 128.
6. MAYES, P. E., G. A. DESCHAMPS, and W. T. PATTON, "Backward Wave Radiation from Periodic Structures and Application to the Design of Frequency Independent Antennas.", Proc. of the I.R.E., May 1961 Volume 49, #5, p. 962.
7. MA, A. T., "Theory and Operation of Antenna Arrays.", John Wiley and Sons, Toronto, 1974. p. 326.
8. RUISEY, V. H., "Frequency Independent Antennas.", Academic Press, N.Y., 1966. pp. 8 - 12.
9. THE AMERICAN RADIO RELAY LEAGUE, "The A.R.R.L. Antenna Handbook.", The American Radio Relay League, Newington, Connecticut, 1974. pp. 160 - 164.

10. JORDAN, E. C. and K. G. BALMAIN, "Electromagnetic Waves and Radiating Systems.", second edition, Prentice - Hall Inc., Englewood Cliffs, N.J., 1968, p. 406.
11. BROWN, R. C. et. al., "Lines, Waves and Antennas -- The Transmission of Electric Energy.", second edition, The Ronald Press Co., N.Y., 1973, pp. 83 - 85.
12. DUNCAN, J. W. and V. P. MINERVA, "100 : 1 Bandwidth Balun Transformer.", Proc. of the I.R.E. #48, 1960., pp. 156 - 164.
13. KLOPFENSTEIN, R. W., "A Transmission Line Taper of Improved Design.", Proc. of the I.R.E. #44, Jan. 1956, pp. 31 - 35.
14. GROSSBERG, M. A., "Extremely Rapid Computation of the Klopfenstein Impedance Taper.", Proc. of the I.R.E. #56 Sept, 1968, pp. 1629 - 1630.
15. BAWER, R. and J. J. WOLFE, "A Printed Circuit Balun for Use with Spiral Antennas.", I.R.E Transactions on Microwave Theory and Techniques, Vol. MTT - 8, May 1960, p. 321.
16. KERNWEIS, N. P., "Log-periodic Antennas: An Experimental Comparison.", Air Force Cambridge Research Laboratories technical report #AFCRL - TR - 75 - 0577, Nov. 4, 1975.
17. RHODES, P. D., "The Log - Periodic Dipole Array.", Q.S.T., November 1973, pp. 16 - 22.
18. CRAVEN, J. H., "A Novel Broadband Balun.", I.R.E. Transactions on Microwave Theory and Techniques, Vol. MTT - 8, Nov. 1960, pp. 672 - 673.

19. SAAD, T. S., R. C. HANSEN and G. J. WHEELER, "Microwave Engineer's Handbook Volume 1.", Artech House Inc., Dedham, Mass., 1971.
20. WHEELER, H. A., "Transmission Line Properties of Parallel Strips Separated by a Dielectric Sheet.", I.E.E.E. Transactions on Microwave Theory and Techniques, Vol. MTT - 13, March 1965, pp. 172 - 185.
21. HAYT, W. H., "Potential Solution of a Homogeneous Strip Line of Finite Width.", I.R.E. Transactions on Microwave Theory and Techniques, July, 1955, pp. 16 - 18.
22. BALMAIN, K. G. and J. NKENG, "Asymmetry Phenomenon of Log Periodic Dipole Antennas.", I.E.E.E. Transactions on Antennas and Propagation, Vol. AP - 24, #4, July 1976, pp. 402 - 410.
23. CAMPBELL, C. K., I. TRABOULAY, M. S. SUTHERS and H. KNEVE, "Design of a Stripline Log - Periodic Dipole Antenna", I.E.E.E. Transactions on Antennas and Propagation, Vol. AP-25, #5, Sept. 1977, pp. 718 - 721.